AD

Report 1921

# FUEL CELL-ELECTRIC PROPULSION TEST RIG

## (MODIFIED M-37, 3/4-TON CARGO TRUCK)

by

Lonnie D. Gaddy, Jr.



February 1968



U. S. ARMY MOBILITY EQUIPMENT RESEARCH AND DEVELOPMENT CENTER

FORT BELVOIR, VIRGINIA



49

U. S. ARMY MOBILITY EQUIPMENT
RESEARCH AND DEVELOPMENT CENTER
FORT BELVOIR, VIRGINIA

Report 1921

# FUEL CELL-ELECTRIC PROPULSION TEST RIG

## (MODIFIED M-37, 3/4-TON CARGO TRUCK)

Task 1C022001A01201

February 1968

Distributed by

The Commanding Officer
U. S. Army Mobility Equipment Research and Development Center

Prepared by

Lonnie D. Gaddy, Jr.
Power Technology Division
Electrotechnology Laboratory

## SUMMARY

This report covers the assembly and test of a fuel cell power plant and associated electric drive system mounted on an M-37, 3/4-ton cargo vehicle.

The report concludes that:

a. The fuel cell and electric drive are adequate for the designed purpose of investigating performance feasibility.

b. The fuel cell-electric propulsion system performs satisfactorily when operated on highways, secondary roads, and grades up to 30 percent.

c. The use of a fuel cell as compared with other power plants such as a battery does not pose additional electrical problems.

d. Major technical advances are required for the fuel cell and the electric drive before all military objectives can be met.

# FOREWORD

Authority for the investigation covered in this report is contained in Project 1L013001A91A 00 039 EF, "In-House Laboratory Independent Research Program," and DA Project 1C022001A012, "Electrical Power Research."

The period covered by this report is from July 1965 to December 1967.

The work was under the direction of T. G. Kirkland, Acting Chief, Electrotechnology Laboratory, and R. E. Hopkins, Chief, Power Technology Division, and was carried out under the supervision of L. D. Gaddy, Jr., with assistance from the Materials Research Support Division, Developmental Fabrication Division, and Advanced Developments Branch of the Power Equipment Division.

Work in support of this investigation was performed, in part, by E. Gillis, R. Chapman, S. Williams, D. Roesler, and G. Sisk of the Electrotechnology Laboratory.

Special recognition is given to Philip Dantowitz of Monsanto Research Corporation and William McMurray of General Electric Company for assistance in various portions of the report.

CONTENTS

ILLUSTRATIONS

ILLUSTRATIONS (cont'd)



TABLES

# FUEL CELL-ELECTRIC PROPULSION TEST RIG

# (MODIFIED M-37, 3/4-TON CARGO TRUCK)

## I. INTRODUCTION

1. Subject. This report summarizes the work conducted during the development and test of a fuel cell-electric propulsion system for an M-37 truck.

2. Background. The history of electric propulsion has been described in several papers. Interest has recently been revived due to the increased energy density of batteries and power density of fuel cells. This in conjunction with improved static conversion devices and techniques, control equipment, and higher energy density rotating equipment provides many attractive features.

The fuel cell and other constant-voltage, direct-current power supplies have been justified on the military basis of either a logistic or special requirement. Little operating data exist on fuel cell-electric propulsion systems. This report describes the vehicle and limited tests conducted.

3. Scope. The design of this equipment was the result of a U. S. Army Engineer Research and Development Laboratories[1] (USAERDL) in-house effort. Tests were conducted at the USAERDL Annex, Fort Belvoir, Virginia. Motion (film number RF 2168) and still photographic coverage of the tests was obtained.

## II. INVESTIGATION

4. Description of Test Rig. The conventional power plant and drive system consisting of engine, transmission, and transfer case were removed from the M-37, 3/4-ton cargo truck and replaced with an electrical propulsion system. Figure 1 shows the fuel cell test rig. The fuel cell-electrical drive consists of three major elements: Fuel cell power plant, motor and vehicle control system, and electric traction motor. Figure 2 shows a block diagram of the electric propulsion system.

1. Now redesignated U. S. Army Mobility Equipment Research and Development Center.

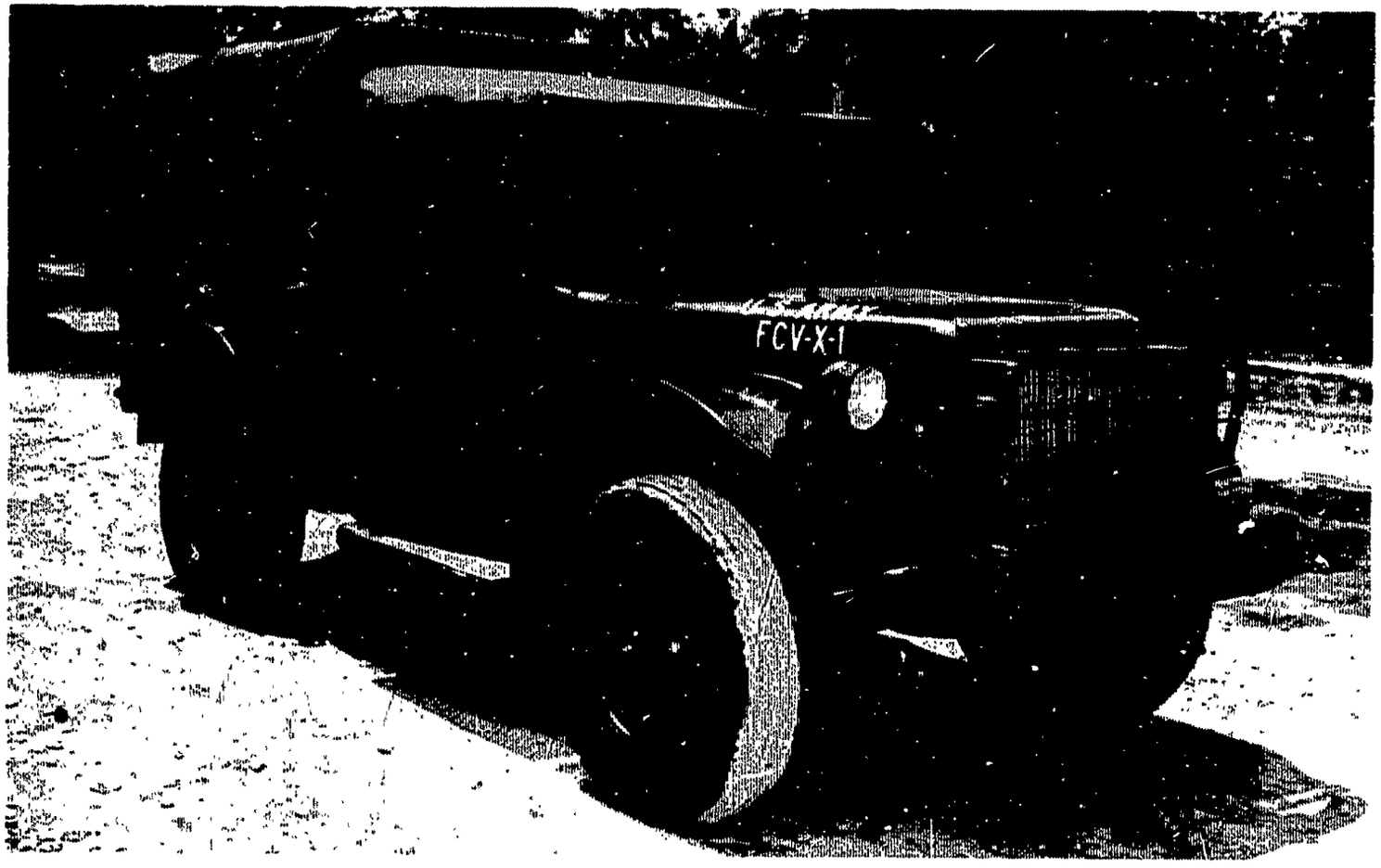


N5949

**Fig. 1. Fuel cell test rig.**

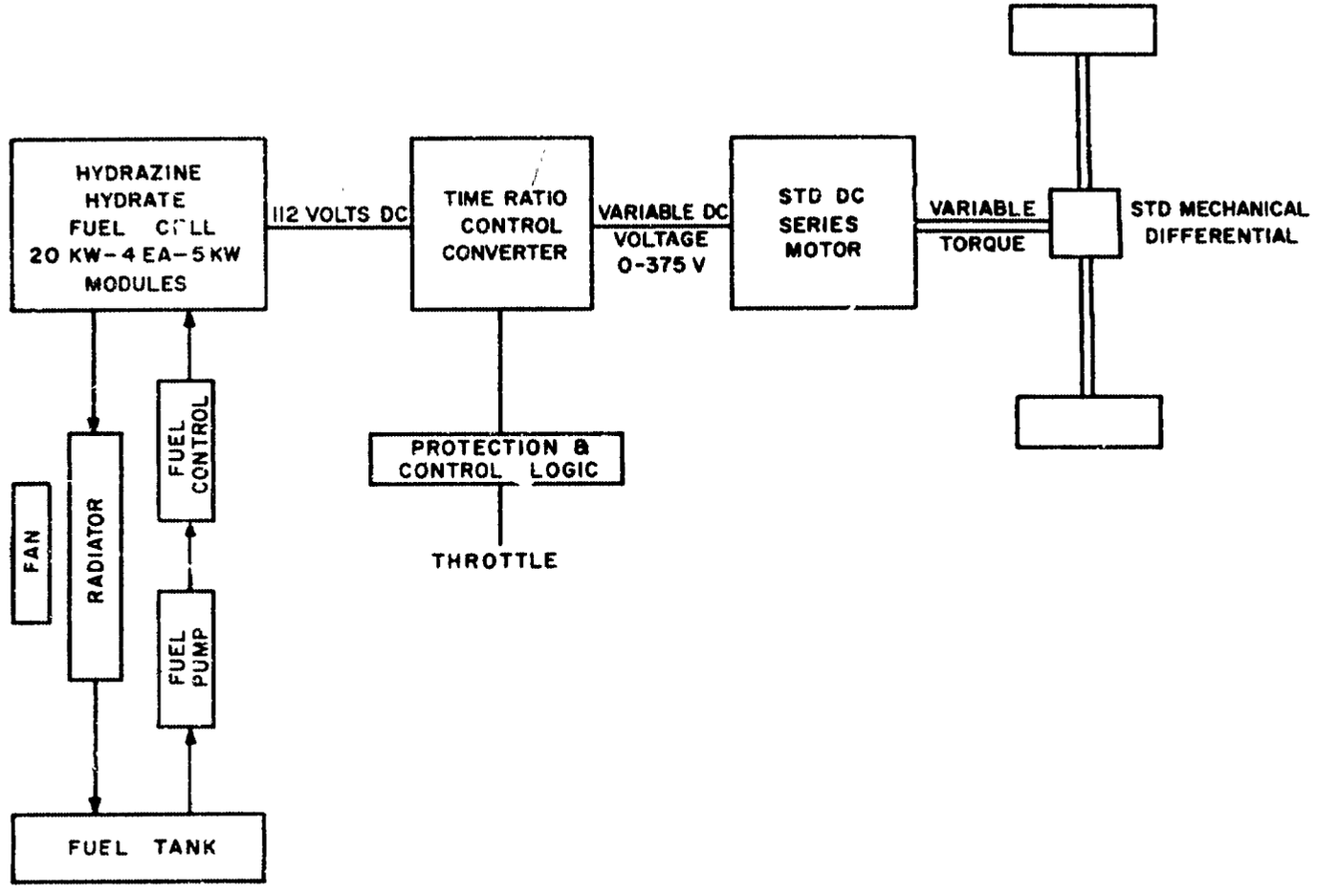


Fig. 2. Block diagram of electric propulsion system.

a. Fuel Cell Power Plant. The fuel cell power plant consists of four 5-kilowatt hydrazine-air modules, heat exchanger and fan, electrolyte pump and reservoir, fuel tank, fuel pump, scrubber, and air blowers. The electrolyte flow through the modules is in parallel as shown in Fig. 3. The four modules are connected in series giving a full load (20 kilowatts) voltage of 112 volts.

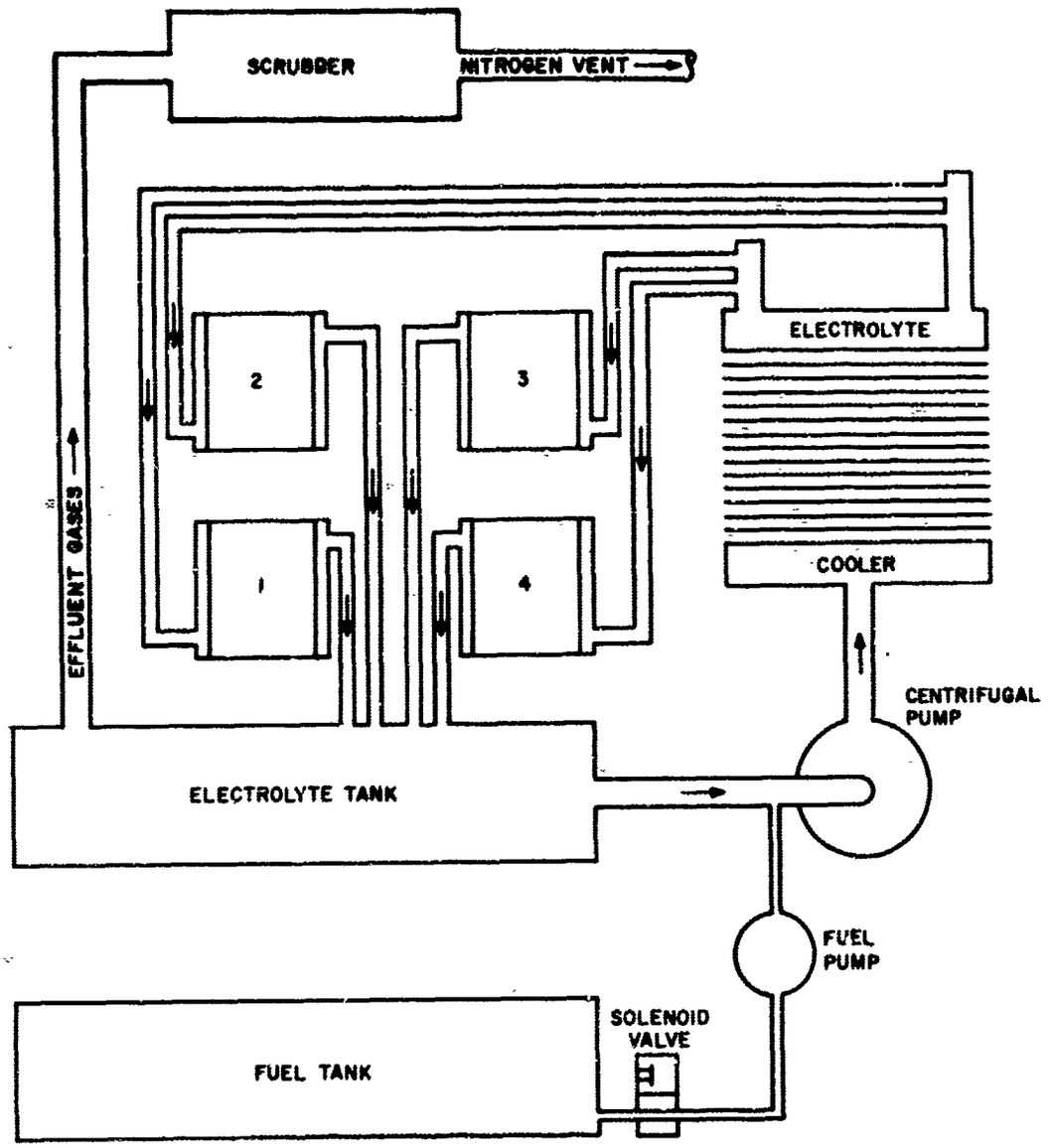


Fig. 3. Twenty-kilowatt electrolyte flow.

(1) Fuel Cell Module. The fuel cell module is designed so that the fuel dissolved in the electrolyte can be circulated through the anode compartments. The circulation rate is high enough so that the electrochemical fuel consumption hardly changes the fuel concentration, even at high load. This circulating liquid also provides the means for cooling the fuel cell. The module itself consists of 140 cells spatially arranged so that anode faces anode (as opposed to bipolar). The anodes are connected electrically in parallel by a metallic grid, the current being brought to the edge of the electrode. Similarly, adjacent cathodes face each other, but in operation they are at different potentials, typically being 0.8 volt apart. An insulating plastic grid is, therefore, incorporated in the cathode compartment. As with the anodes, the cathode current is collected and brought to the edge of the electrode. Suitable external electrical connections are made so that each pair of cells (one cell being one cathode and one anode) is in series with the next, and appropriate cathodes are in parallel. Figure 4 shows a schematic of the arrangement and the external electrical connections. The module consists

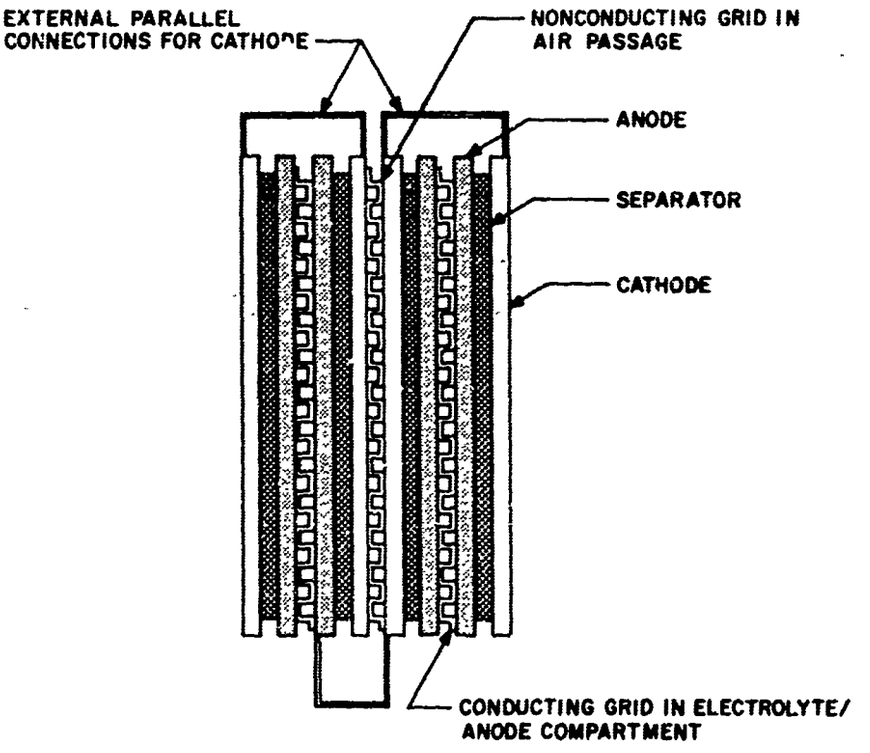


Fig. 4. Module component assembly.

of two side-by-side decks of 70 cells each, connected in parallel electrically and clamped between common end plates. At rated load, each cell is designed to deliver 0.8 volt. Since each pair of cells is wired in parallel, the rated voltage of the module is 28 volts. Each electrode has an active area of 62 square inches, and is rated at 44.5 amperes at a rated current density of 103 amperes per square foot. Two cells in parallel deliver 89 amperes, which is the current carried by each deck. Twin decks in parallel carry 178 amperes at 28 volts, yielding a 5-kilowatt rating. The module is shaped like a box, with overall dimensions of 9 by 9 by $22\frac{1}{2}$ inches and weighing 95 pounds with electrolyte. At the 5-kilowatt rating, the power density is 4.38 kilowatts per cubic foot and the specific weight is 19 pounds per kilowatt. Under design conditions, about 700 watt-hours are generated per pound of hydrazine monohydrate (about 90 percent of ideal). Figure 5 shows the average single cell polarization curve, based on module tests.

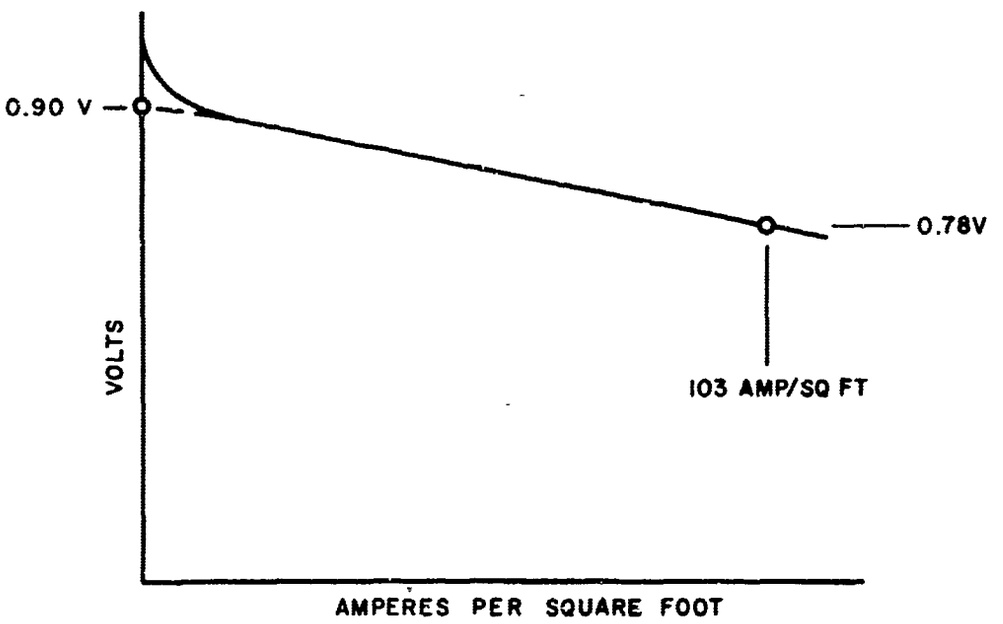


Fig. 5. Volt-ampere load line.

At rated power, the average single cell voltage is 0.78 volt, which is about 48 percent of the thermodynamically reversible voltage for the hydrazine/oxygen couple. Thermal efficiency at this condition is about 50 percent, based on the higher heating value of hydrazine.

The hydrazine-air fuel cell generates gases which contain a significant amount of ammonia. A scrubber containing cupric sulfate solution was installed to absorb the ammonia. The amount of solution required is discussed in paragraph 5a.

(2) Fuel Cell Auxiliaries. The weight of electrolyte required to charge the system is 100 pounds. The radiator, which is in an air-to-electrolyte heat exchanger, weighs 45 pounds. The latter is a finned, tube radiator, similar to those found on many American cars. To enhance ram air cooling, an electric motor drive fan is provided. The fan is thermostatically controlled, being on only when the electrolyte temperature has risen above a preset value. The electrolyte is circulated through the fuel cell and the radiator by a motor-driven centrifugal pump. Fuel is supplied by a pump to the electrolyte tank in an intermittent fashion, the flow being either on or off. The "on" versus "off" time of the fuel flow determines the average quantity of fuel delivered. This, in turn, is regulated by the voltage on the terminals of one of the modules. Parasitic power drain for the 20-kilowatt system is about 600 watts. Off-the-shelf components were used with limited concern for noise level or weight.

The auxiliaries are required to maintain the following operational parameters:

Operating temperature: $60^{\circ}$ C maximum.

Electrolyte flow: 2.5 gallons per minute per module minimum.

Maximum hydraulic pressure: 2.5 pounds per square inch (gage) at inlet.

Hydrazine concentration in electrolyte: 0.5 molar minimum to 2.5 molar maximum.

Air flow rate: 20 cubic feet per minute per module minimum.

Electrolyte composition: $5 \pm 1$ molar KOH.

Electrical load: 180-ampere maximum average continuous current and 280-ampere maximum instantaneous current.

Contaminants: Caution should be used to prevent entry of extraneous chemical compounds into the modules on air or liquid side. Sulfur in every form should be particularly guarded against. Sulfur-free components are essential.

b. Secondary Batteries. In order to investigate the advantages and disadvantages of batteries and to evaluate the control requirements for hybrid operation, the test rig was equipped with lead-acid batteries. With the batteries mounted in the rear, the test rig was operated with 20-kilowatt power from the fuel cell and 20-kilowatt power from the batteries. A silicon rectifier prevented a power flow from the batteries to the fuel cell as shown in Fig. 6. The lead-acid batteries were discharged at a 300-ampere rate corresponding to six times the nominal ampere-hour capacity. Nickel-cadmium batteries discharged at a 300-ampere rate corresponding to 18 times the nominal ampere-hour rating were used in lieu of the lead acid. Figure 7 shows the nickel-cadmium battery installation.

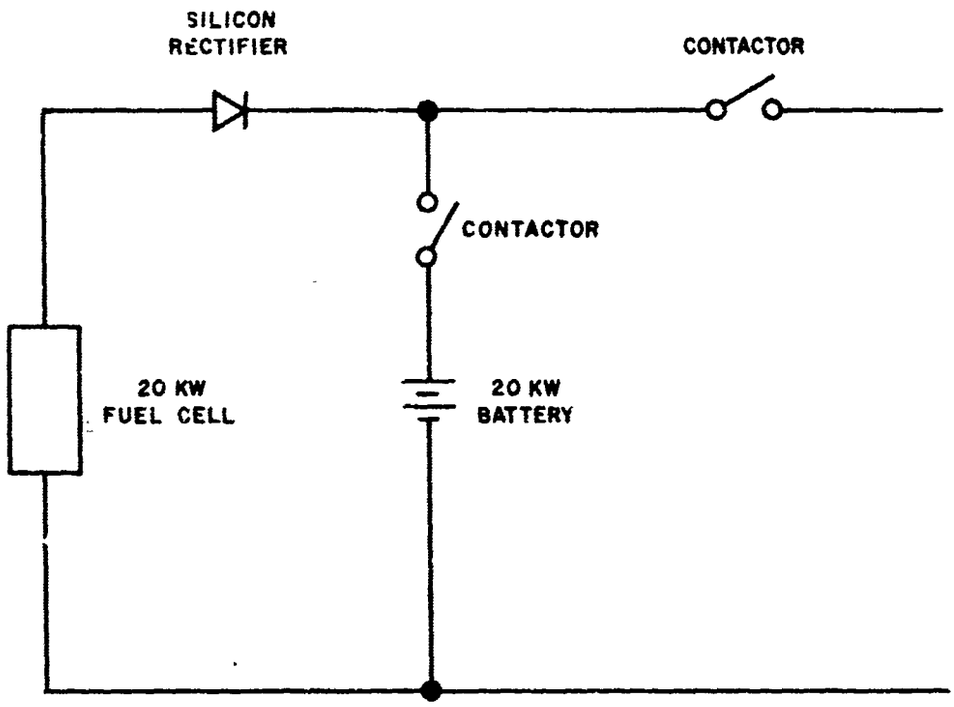


Fig. 6. Hybrid power plant schematic.

c. Static Controller.

(1) Description. The static controller is rated at 40 kilowatts input from either a nominal 224- or 112-volt direct current, and with an output voltage continuously adjustable from 0 to 375 volts direct current. This requires three modes of operation: Step-down

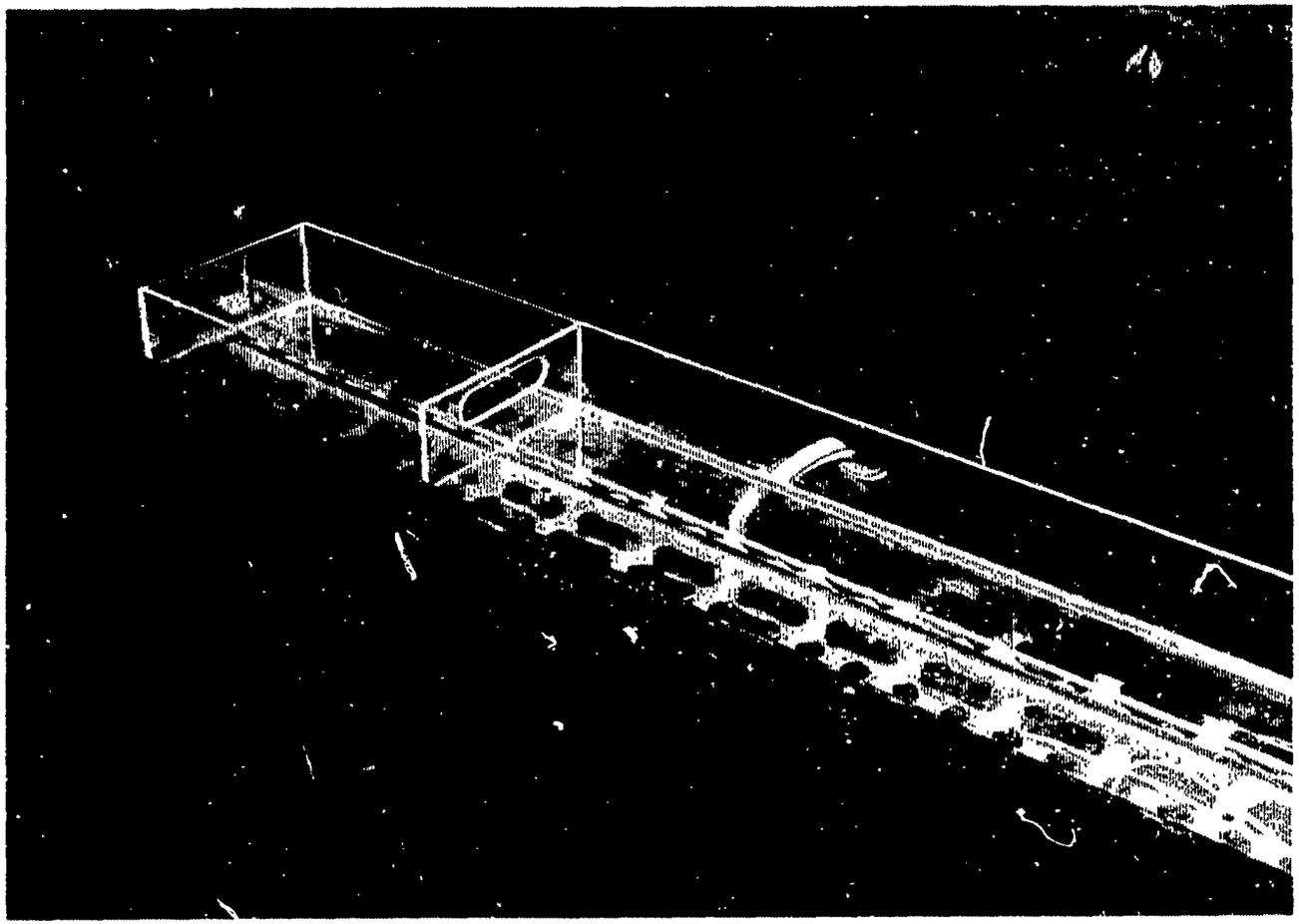

P4752

Fig. 7. Nickel-cadmium battery installation.

when the output voltage is lower than the input, straight-through when they are equal, and step-up when the output is higher. The controller has been designed to act as a matching device between a 40-kilowatt power source and a series direct-current traction motor.

The controls of the circuit are so arranged that only an accelerator pedal operated in the conventional manner is required to safely and smoothly control the vehicle between any operating points within the established boundary conditions. Limit circuits are provided that prohibit at any time exceeding a 20-kilowatt output of the fuel cell, 527-ampere input to the motor, 375-volt input to the motor, and 3,600 revolutions per minute speed of the motor.

Minor differences in sensing, power, and control circuitry are required to change operation from one input voltage to the other. The basic difference in the limit conditions is a maximum 180-ampere average fuel cell current with the 224-volt input, and 360-ampere average with the 112-volt input. In all cases, the circuit is required to operate at rated current input with an input voltage tolerance of +0, -15 percent.

The circuit is not required to provide for reverse flow of current; therefore, it cannot be used for dynamic or regenerative braking. To prohibit plugging, controls are provided that prevent the field of the motor from being reversed while the vehicle is moving. Incorporated in this control is a safety overspeed circuit that trips the power contactor in the event the motor overspeeds to 3,750 revolutions per minute.

(2) Operation. This description of operation is written with reference to the basic power circuit diagram shown in Fig. 8, where single silicon controlled rectifiers (SCR's) and diodes are shown instead of the actual parallel pairs, and certain accessory components are omitted for simplicity.

The commutating capacitor C and its charge-reversing circuit, $SCR_C$ and inductance $L_C$, are common to both the step-down and step-up portions of the controller. Between the commutating intervals, capacitor C is charged with the polarity indicated in Fig. 8. An auxiliary circuit (not shown in Fig. 8) provides this charge when the main contactor is first closed to energize the circuit, and at other times when the load current is too small to charge C.

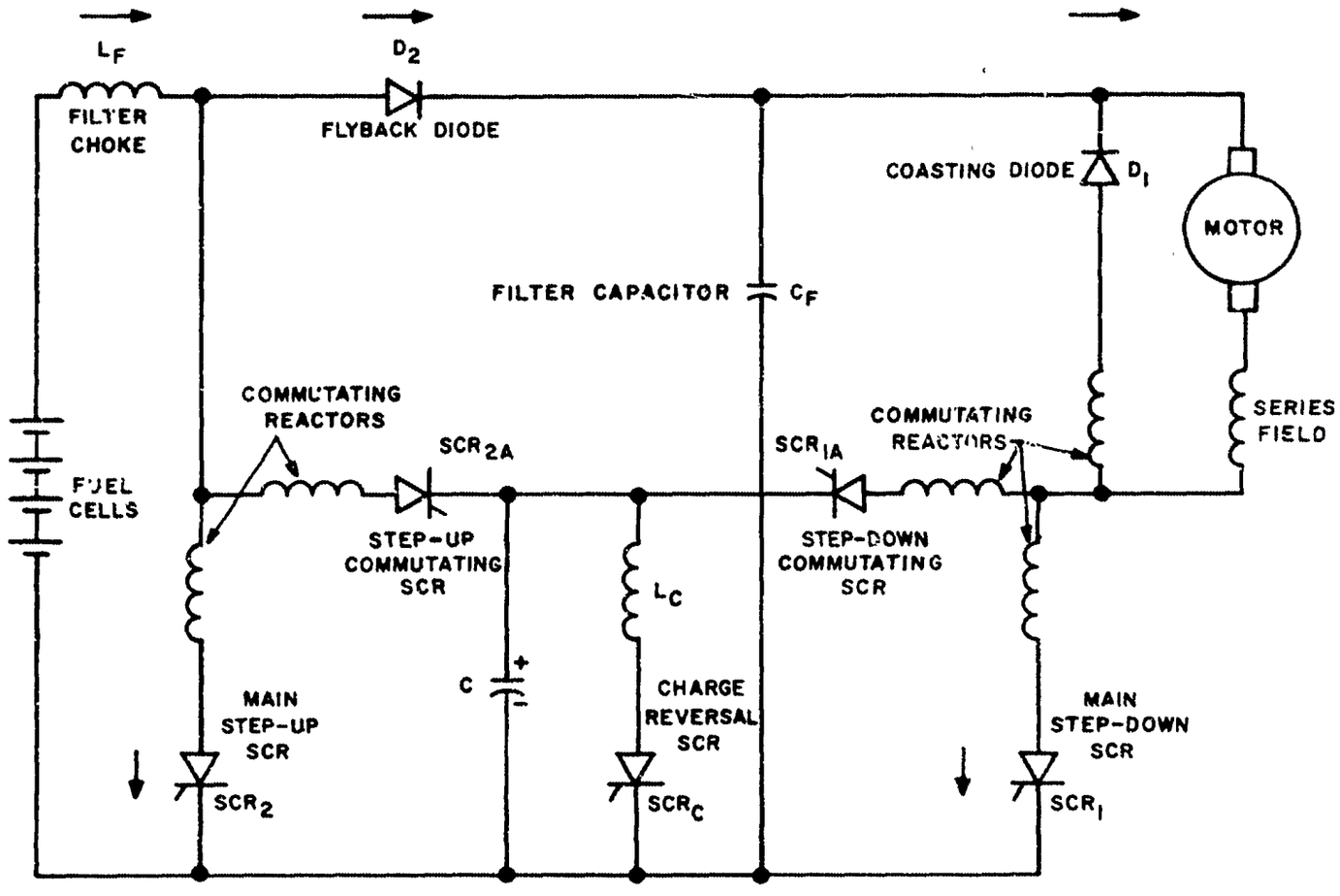


Fig. 8. Basic power circuit diagram.

During step-down, $SCR_2$ and $SCR_{2A}$ are not fired and are not active, and the current in diode $D_2$ is the same as in the fuel cell. The filter choke $L_F$ and capacitor $C_F$ smooth the pulses of current drawn by the step-down chopper.

A cycle begins when $SCR_1$ is fired, drawing current from the supply through the motor. The "on" time of $SCR_1$ is determined by the control circuit as a function of the throttle setting. To begin the process of commutation or turning off $SCR_1$, the auxiliary $SCR_C$ is fired. Capacitor C discharges through inductance $L_C$ and recharges with reverse polarity. Since the loop C, $L_C$, $SCR_C$ has a short time constant, the final reverse voltage on C is only slightly less than the initial forward voltage. As soon as the current in $L_C$ becomes zero, the reverse voltage turns off $SCR_C$.

Auxiliary $SCR_{1A}$ is fired a short time after the trigger is applied to $SCR_C$. This time delay allows the charge reversal to be completed. The reverse voltage on C is now applied to $SCR_1$, turning it off. The load current continues to flow through the motor, $SCR_{1A}$, and capacitor C until C is charged to the supply voltage, at which time diode $D_1$ conducts. During the "off" time of $SCR_1$, the load current coasts through $D_1$, being maintained by the motor inductance.

The commutating reactors serve to limit the rates of rise and fall of current in the power devices $SCR_1$, $D_1$, and $SCR_{1A}$. These reactors also aid the R-C filters which are connected across those power devices (not shown in Fig. 8) in limiting the voltage spikes caused by switching. The current trapped in the reactors after commutation (when $D_1$ beings to conduct) causes the commutating capacitor C to overcharge by an amount proportional to the load current.

In the straight-through mode, $SCR_1$ is turned on and left on. Current flows from the fuel cell through $L_F$, $D_2$, the motor, and $SCR_1$. $SCR_C$ and $SCR_{1A}$ are not fired, and capacitor C remains charged with the polarity indicated in Fig. 8, ready to start a commutating cycle for $SCR_1$ when the throttle setting is reduced.

During step-up, $SCR_1$ is turned on and left on; $SCR_{1A}$ is not fired and remains inactive. To start a step-up cycle, $SCR_2$ is fired, short-circuiting the fuel cell through the choke $L_F$. Current builds up linearly, storing energy in the choke. During this on time of $SCR_2$, diode $D_2$ is blocking, while the motor current is supplied by filter capacitor $C_F$.

The commutation or turnoff process for $SCR_2$ begins with firing $SCR_C$ to reverse the charge on capacitor C in the same manner described for the step-down mode. After a short time delay, $SCR_{2A}$ is fired to apply the reversed capacitor voltage to $SCR_2$, thereby turning it off. Current continues to flow from the fuel cell through $L_F$ and $SCR_{2A}$ to charge C up to the voltage on $C_F$, at which time diode $D_2$ again conducts. The extra energy stored in $L_F$ is now delivered into filter capacitor $C_F$, charging it higher than the fuel cell supply voltage.

Figure 9 shows the static controller mounted under the operator's seat. Because of limitations of the available SCR's and the capability of voltage step-up as well as step-down, the magnetic portion of the controller necessitates a total controller weight of 300 pounds.

d. Traction Motor. The traction motor is a Model GE-1244A four-pole, direct-current, series-wound, self-ventilated, commutating pole type. The motor is mounted under the operator's seat forward of the differential which it drives. The motor is rated at a stall torque of 525 foot-pounds when supplied by a current of 500 amperes. The stall torque is a short time rating only. The motor weighs 700 pounds and was selected based solely on its availability. The maximum permissible motor speed is 3,600 revolutions per minute. Figure 10 shows the motor mounted on the test rig.

e. System Controls. It became apparent as the test rig developed that it would be convenient to package much of the vehicle control in the same package with the static controller.

Figure 11 is a schematic of the operating and limit controls for the test rig. The main contactor (K1) and reverse (K2) are interlocked so that two conditions must occur simultaneously before closure: The vehicle must not be moving, and the accelerator pedal must not be depressed. This requirement is to insure that the reverser, which is a low-voltage device, will not close under load. The opening process is the same in reverse.

The controller insures that neither the operator demand nor motor load shall exceed the power capability of the fuel cell. Figure 12a shows how motor current, voltage, and power vary as a function of vehicle velocity following a full-throttle start from a standstill. Figure 12b shows the fuel cell voltage and current on the same scale. In the span

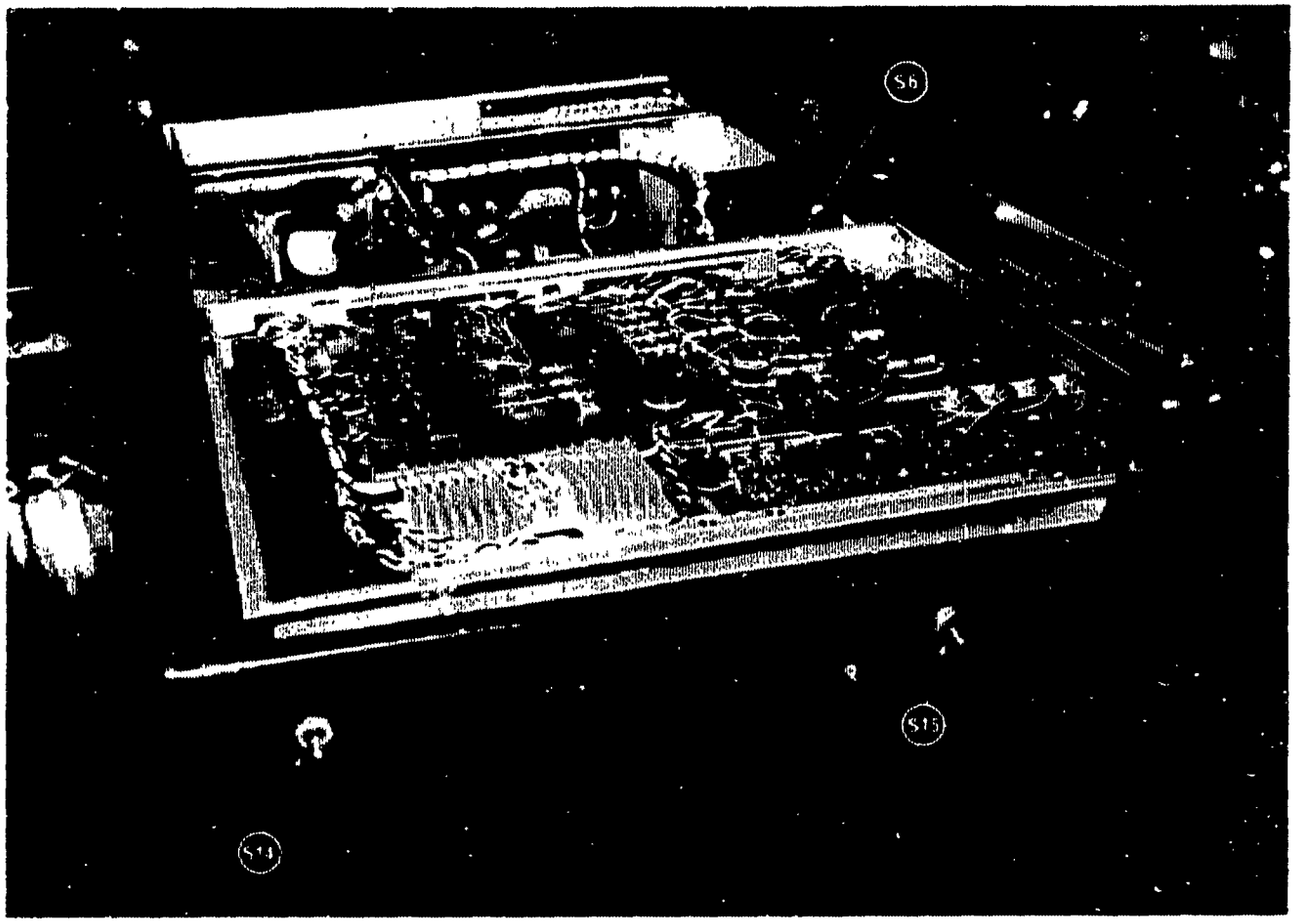


P4749

**Fig. 9. Static controller mounting. (Callouts indicate switch designations and locations.)**

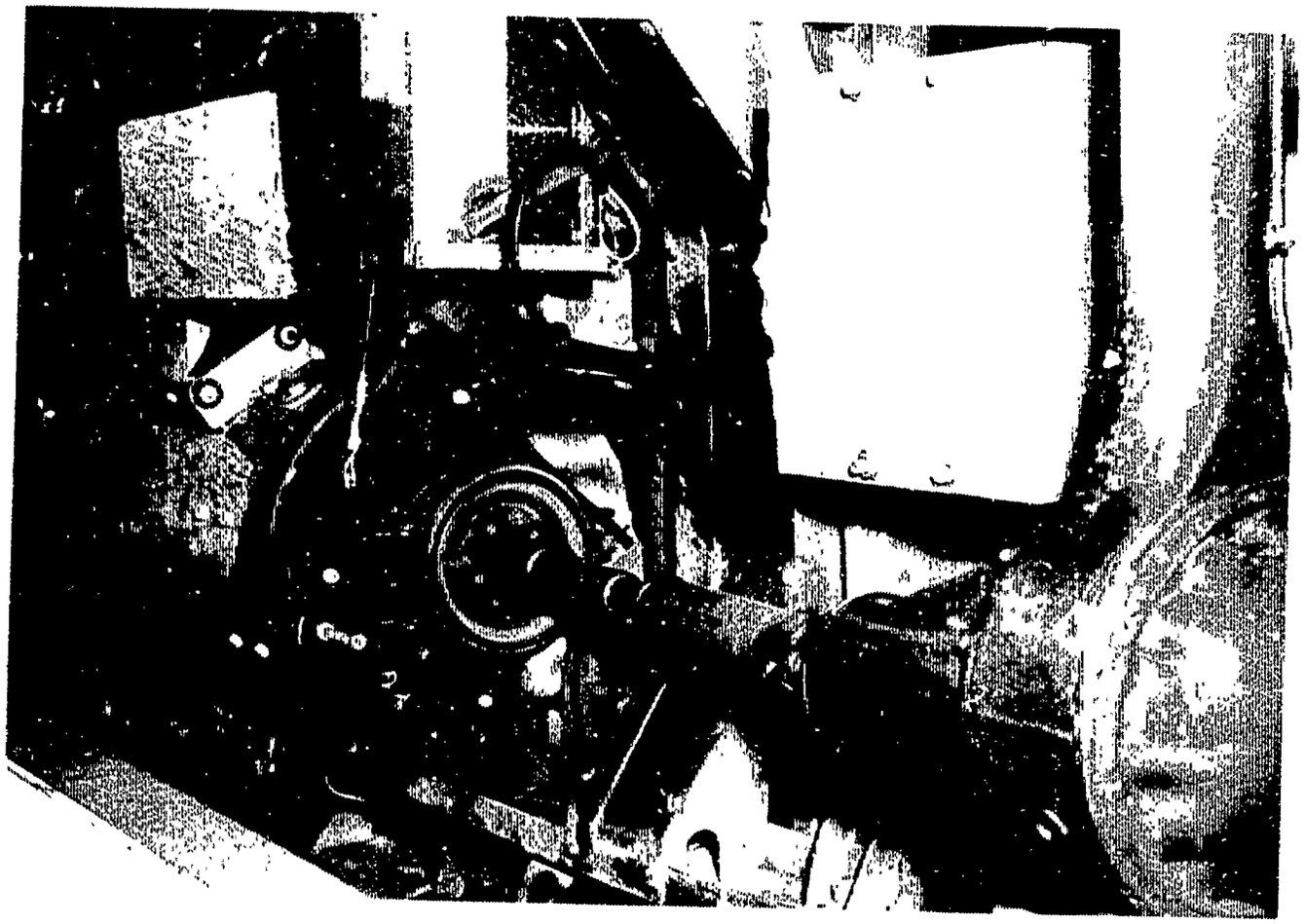

P4785

Fig. 10. Traction motor mounting.

marked "A," the controller limits the current to the motor to 525 amperes. Since the short-circuit current of the fuel cell is 2,500 amperes, protection is clearly required. As the vehicle and the motor pick up speed, motor voltage is increased to maintain the current limit. At the end of span A, the motor power is equal to 40 kilowatts, which is equal to the peak power plant power. During the span marked "B," the vehicle continues to accelerate and the motor back E. M. F. continues to increase, requiring a higher voltage and a lower current to maintain constant power. Note that during span B the motor voltage is first below and then above the power source voltage, requiring a controller with both step-down and step-up capabilities. At the beginning of span C, the vehicle has reached its maximum speed, and no further change in voltage, current, or power occurs.

The main contactor will open if the motor speed exceeds 3,750 revolutions per minute in the forward direction or 1,400 revolutions per minute in the reverse direction.

f. Instrument Panel. The instrument panel is shown in Fig. 13. The switch designations are referenced to the simplified schematic shown in Fig. 14.

The meters shown on the instrument panel inform test personnel of the important electrical operating conditions and may be replaced by warning lights as operating confidence is established. The temperature indicator shows the operating temperature of the fuel cell end plate. The electrical speedometer indicates vehicle speed in miles per hour. The 0- to 50-volt fuel cell meter is used to monitor individual module voltage as selected by the adjacent rotary switch. Additional meters are provided to indicate total fuel cell voltage, total power supply current, motor voltage, and motor current. The odometer mounted on the left rear wheel indicates total miles traveled.

g. Startup Procedure. The vehicle control schematic shown in Fig. 11 provides all the electric circuitry excluding the static controller described in paragraph 4c.

The following startup procedure is written with reference to the simplified schematic shown in Fig. 14, where certain accessory components are omitted for simplicity.

(1) Close knife switch S6 to RUN position. This connects the 24-volt auxiliary battery to the low-voltage bus.

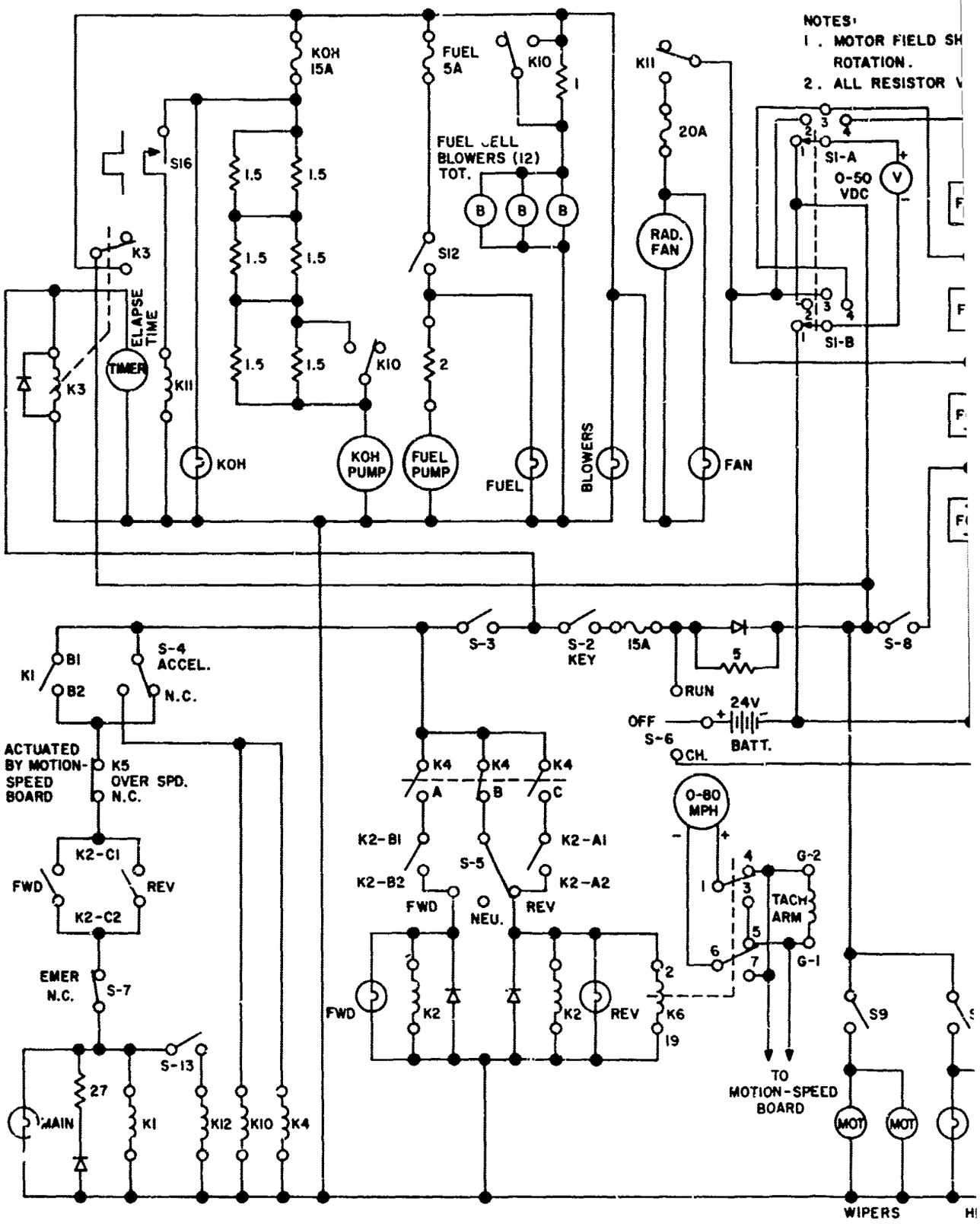
NOTES:
1. MOTOR FIELD SH
ROTATION.
2. ALL RESISTOR
KOH 15A
FUEL 5A
K10
K11
20A
SI6
1.5
FUEL CELL BLOWERS (12) TOT.
B
RAD. FAN
SI-A
0-50 VDC
V
K3
SI2
ELAPSE TIME
TIMER
SI-B
2
KOH
KOH PUMP
FUEL PUMP
FUEL
BLOWERS
FAN
S-3
S-2 KEY
15A
S-8
RUN
OFF
24V
BATT.
S-6
CH.
K1
B1
B2
S-4 ACCEL.
N.C.
ACTUATED BY MOTION-SPEED BOARD
K5 OVER SPD. N.C.
K4
A
B
C
K2-B1
K2-A1
K2-B2
K2-A2
S-5
FWD
NEU.
REV
0-80 MPH
G-2
G-1
TACH ARM
K2-C1
K2-C2
EMER N.C.
S-7
S-13
27
MAIN
K12
K6
19
TO MOTION-SPEED BOARD
S9
MOT
WIPERS

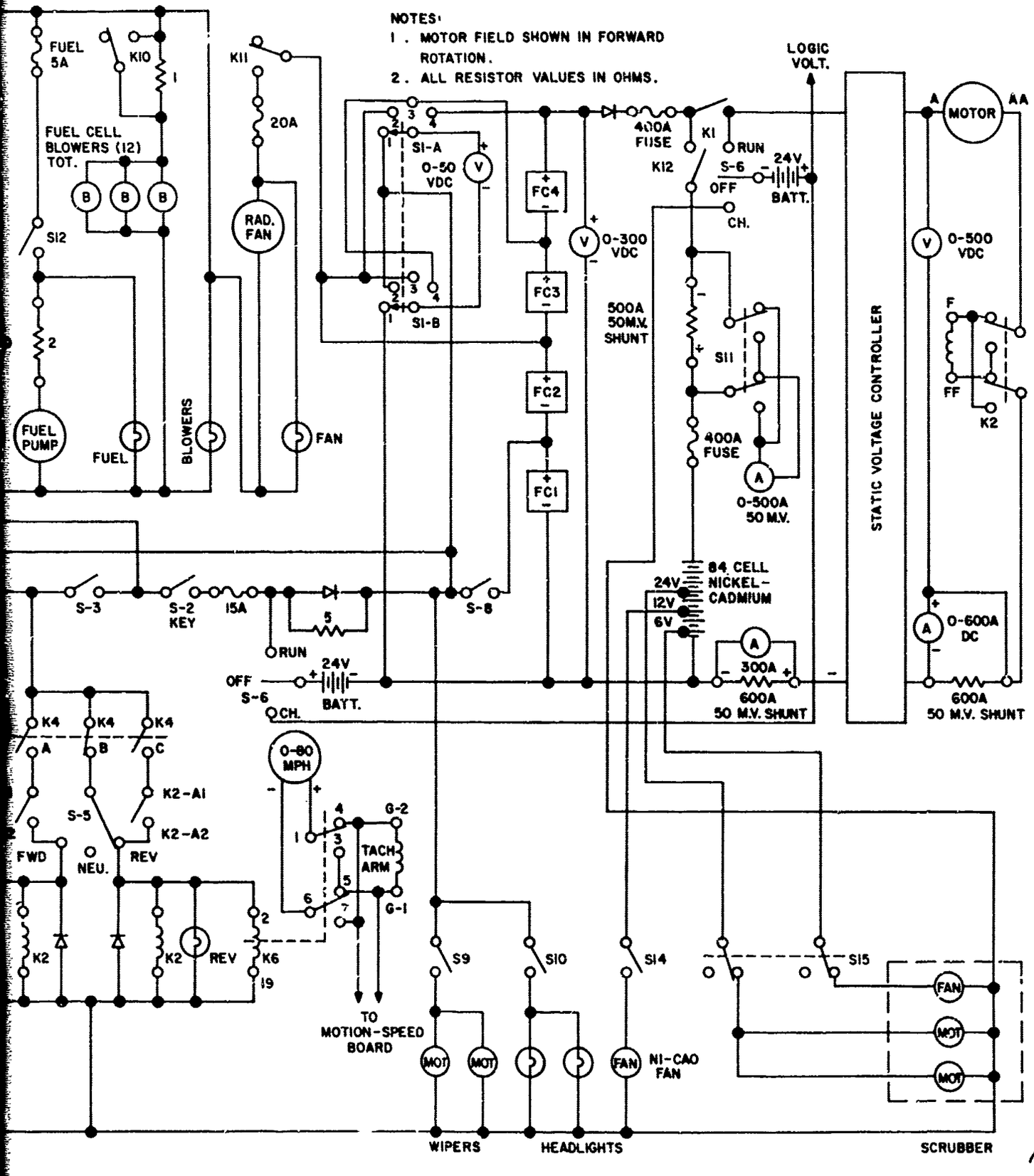


Fig. 11. Vehicle control schematic.

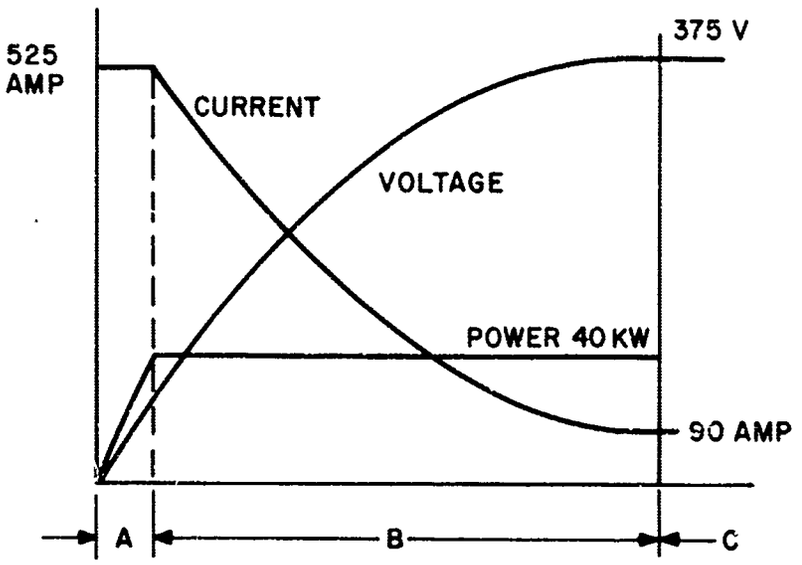


(a)

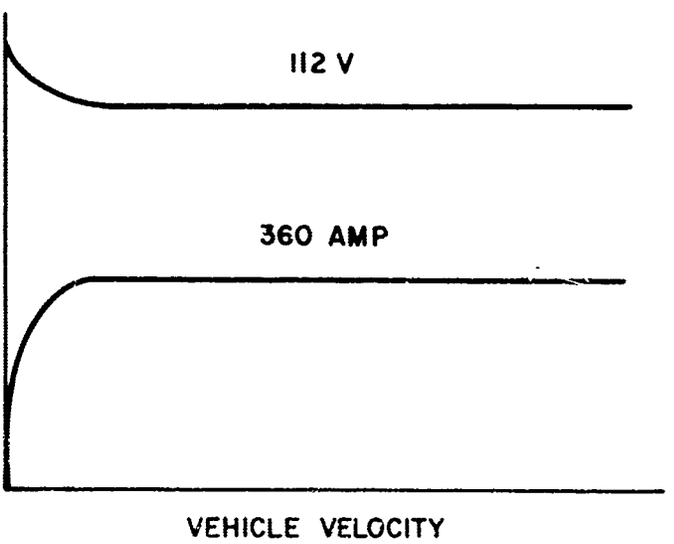


(b)

Fig. 12. Power versus speed curves.

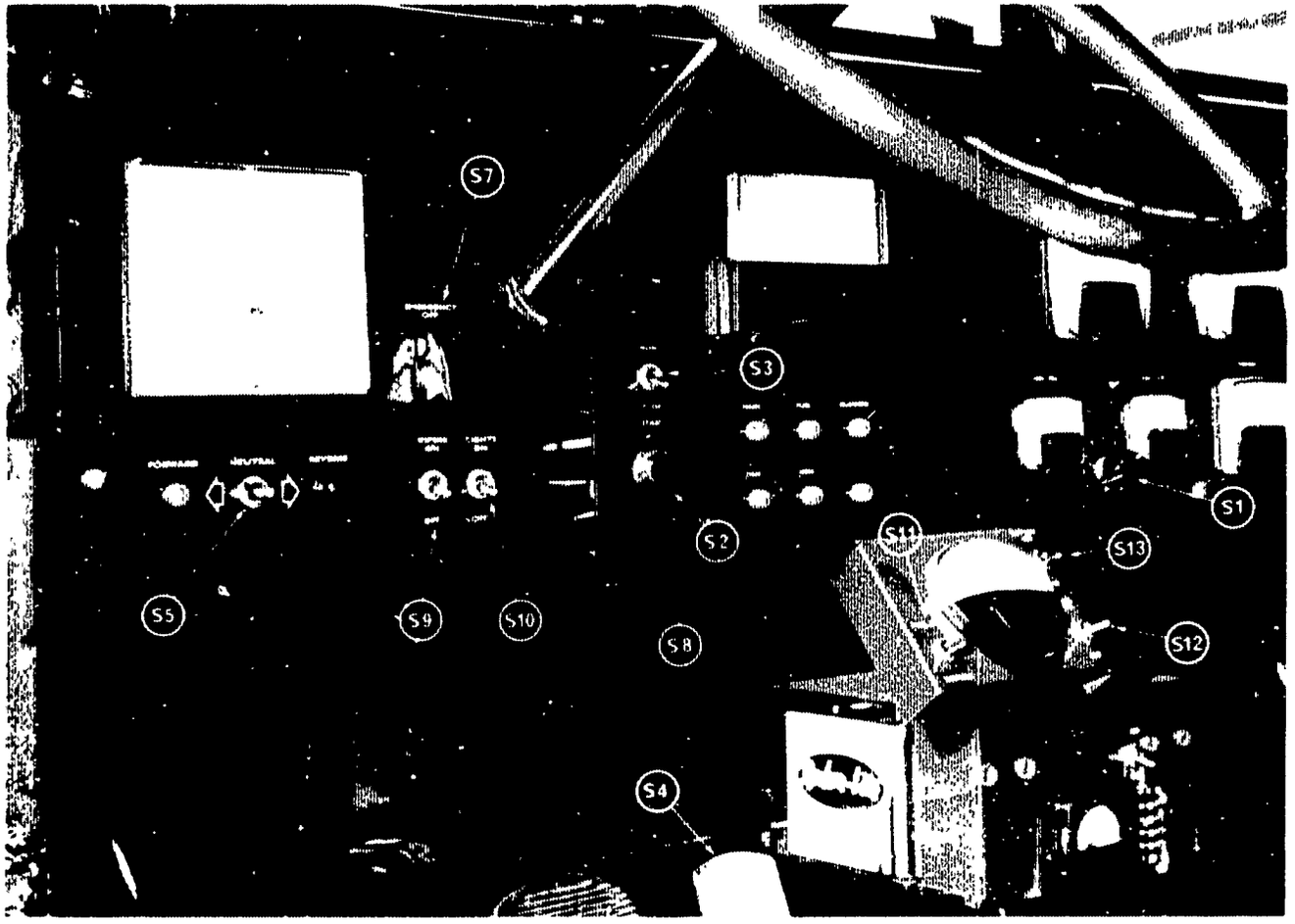


P4748

Fig. 13. Instrument panel. (Callouts indicate switch designations and locations.)

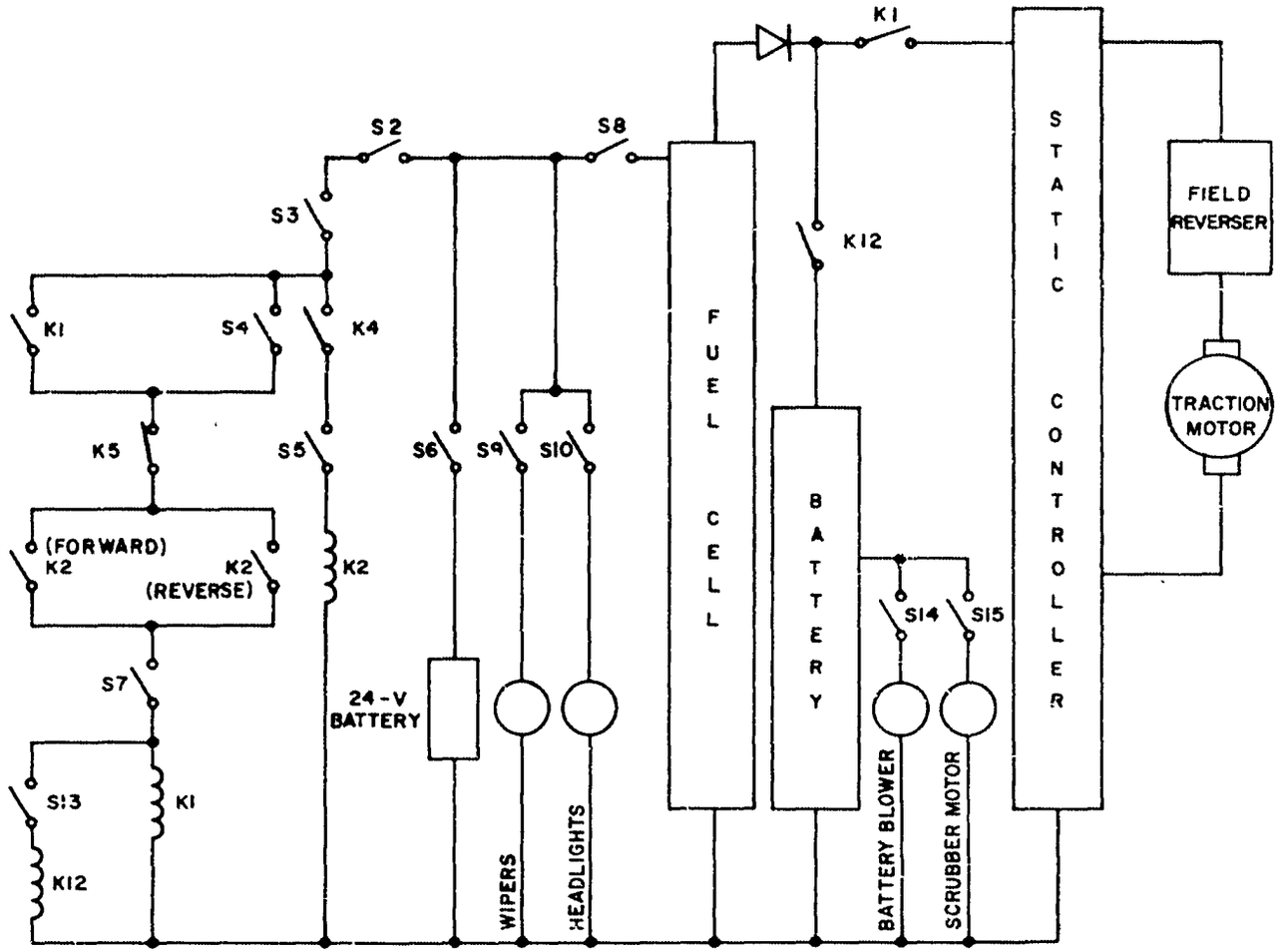


**Fig. 14. Simplified schematic of startup controls.**

(2) Close key switch S2. This energizes KOH pump, fuel cell blowers, and associated indicating lights.

(3) Close RUN STOP switch S3 to RUN position. This switch connects the auxiliaries and interlocks, required for the electric drive system, to the 24-volt auxiliary bus.

(4) Depress accelerator pedal S4. This switch connects the KOH pump and fuel cell blowers to a higher voltage for startup. After the fuel cell voltage is up to 105 volts, the accelerator pedal should not be depressed unless vehicle movement is desired.

(5) Close knife switch S8 after voltage of fuel cell module number 1 is above 25 volts. This connects fuel cell module number 1 to the 24-volt auxiliary battery for battery charging. The total fuel voltage should exceed 110 volts before continuation of startup procedure.

(6) Close FWD-NEU-REV switch S5 to the position of anticipated travel. This closes the main contactor K1 and traction motor field reverser K2. A 1-second delay is built into the reverser to prevent immediate switching from forward to reverse or vice versa. A motion interlock is provided to prevent plugging of the motor. This switch must remain in the NEU position during idle periods.

(7) In case of emergency, such as voltage control failure when vehicle is in motion, close EMERGENCY OFF switch S7. This bypasses motion interlock and opens main contactor K1.

(8) When it is desired to use the scrubber, close switch S15. This energizes both the scrubber motors and fans. The manual flapper valve at the scrubber input should be coordinated for proper operation.

(9) During hybrid, battery only, or battery charging operation, toggle switch S14 must be closed. This switch energizes a small fan in the battery compartment to prevent hydrogen buildup.

(10) Toggle switches S9 and S10 energize the windshield wipers and headlights, respectively.

h. Shutdown Procedure. After FWD-NEU-REV switch S5 is switched to the NEU position, the shutdown procedure is the reverse order of the startup procedure.

i. Safety Precautions. The following are recommendations and cautions in certain areas where safety hazards to personnel and possible equipment damage may occur.

(1) To avoid chemical damage to personnel servicing the fuel cell and auxiliaries, the operator should read information pertaining to care and handling of hydrazine, potassium hydroxide, copper sulfate, ammonia, and hydrogen.

(2) To avoid potential shock hazard to personnel servicing the fuel cell, a 3-ohm, 200-watt bleed resistor should be connected across the fuel cell when not operational.

(3) To avoid pump damage, the fuel and electrolyte level should be checked before operation.

(4) To avoid potential shock hazard to personnel servicing the controller, bleed resistors should always be connected across the commutating capacitor C and across the electrolytic capacitor bank $C_F$ (see Fig. 8).

(5) The housing of the controller and of the electrolytic capacitor bank should always be grounded with a safety ground to avoid shock hazards and flash burns from shorting with tools in the event of loss of insulation in the controller.

(6) A fuse and a manual disconnect protect the power cables between the fuel cells and the static controller since the fuses in the controller will not protect the supply. The disconnect switch should be used before disconnecting cables to protect against shocks and flash burns if the ends of the cables are shorted or touch the truck.

(7) A "crowbar" is installed to blow the fuse cited in the preceding paragraph in the event the controller should experience a failure in the step-down SCR's. This condition would connect the motor directly across the fuel cell. This precaution is suggested since the main contactor will be called upon to operate with a highly inductive load at high current and could conceivably fail. This would result in a runaway condition.

(8) The overspeed trip should always be connected to protect against broken universal or drive shaft or against the controller speed limit failing to protect. The motor is mounted directly under the seat, and a runaway condition of an unloaded series direct-current motor could cause serious injury if the motor fails at high speed.

5. Vehicle Tests. Various tests have been conducted on the test rig. The tests described cover operation over a wide range of load conditions.

a. Ammonia Concentration Test. A test was conducted to determine the amount of ammonia at various locations around the test rig. Figure 15 shows the location and concentration measured with a Scott tester (Drager). The nose is able to detect ammonia concentration as low as 10 to 15 parts per million. The maximum allowable concentration stated in "Dangerous Properties of Industrial Materials" is 100 parts per million.[2]

Plastic ducting was installed to direct all effluent gases to a scrubber containing copper sulfate solution. The scrubber was located

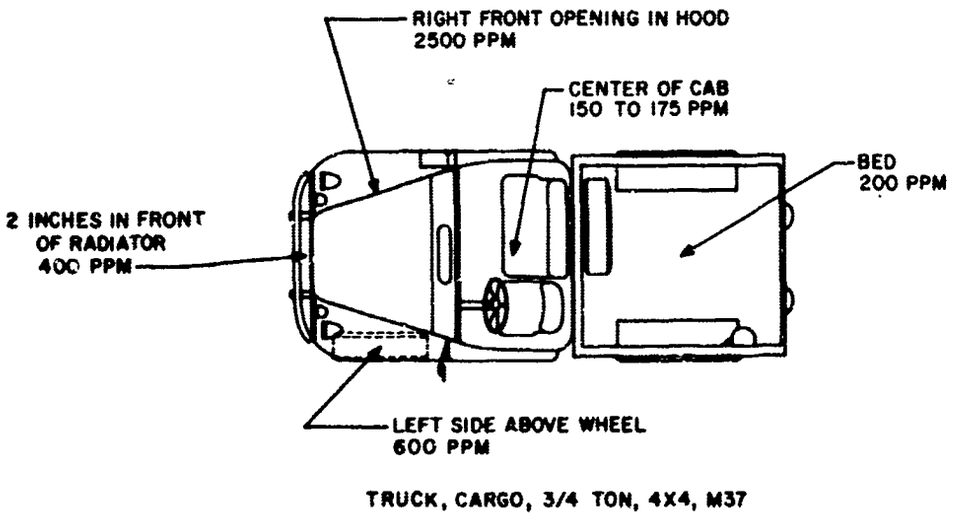


Fig. 15. Ammonia concentration test layout.

2. N. Irving Sax, assisted by Leonard J. Goldwater and others, Dangerous Properties of Industrial Materials, Second Edition, Reinhold Publishing Corporation, New York, 1963, Library of Congress Catalog No. 63-20370.

beneath the test rig bed. At present, 17 pounds of cupric sulfate dissolved in 7 gallons of water absorbs the ammonia effluent for approximately 40 minutes.

b. Power Test 1. Power test 1 covered a test course from USAERDL to USAERDL Annex. At the annex, the test rig was operated on the paved track, dirt track, and several grades ranging from zero to 30 percent. Table I shows the voltage, current, power, and speed for 13 operating conditions. After completion of the test, the vehicle was driven back to USAERDL. The total course covered 22.1 miles with the vehicle in an idle condition for extended periods of time. It should be noted that the maximum power from the fuel cell was 18.0 kilowatts. This was because the fuel cell voltage dropped to 95 volts in lieu of the design value of 112 volts. Ten gallons of fuel was consumed over the course for a specific fuel consumption of 2.21 miles per gallon. This low value was attributed to the inability to control fuel concentration within proper limits. Based upon the results of this test, a fuel controller has been installed, and improved performance has subsequently been obtained.

c. Hybrid Power Acceleration Test. A 20-kilowatt fuel cell and a 20-kilowatt lead-acid battery as shown in Fig. 6 were used in the hybrid power acceleration test. The acceleration test as shown in Fig. 16 was conducted on a limited length track so that the maximum speed was not attained. The curve shows that the fuel cell test rig was in front of the conventional truck up to a velocity of 45 miles per hour. The hybrid power plant provides an improvement in regulation and speed of response when compared with the fuel cell only.

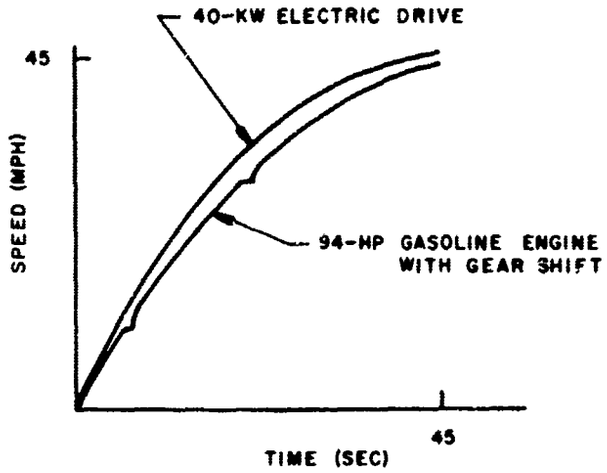


Fig. 16. Vehicle acceleration test.

Table I. Power Test 1 Data

| Location Where Measurement Was Taken | Fuel Cell Output | | | Motor Input | | | Vehicle Speed (mph) |
|---|---|---|---|---|---|---|---|
| | Voltage | Current (amp) | Power (kw) | Voltage | Current (amp) | Power (kw) | |
| Backlick Rd. (Curve at Pohick) | 100 | 150 | 15.0 | 150 | 100 | 15.0 | 26 |
| Backlick Rd. (Straight - Flat) | 105 | 150 | 15.35 | 155 | 95 | 14.7 | 30 |
| Backlick Rd. (Airport Entrance) | 105 | 150 | 15.35 | 170 | 80 | 13.6 | 36 |
| Backlick Rd. - Telegraph Rd. | 95 | 185 | 17.6 | 160 | 100 | 16.0 | 32 |
| Backlick Rd. (Over RR Crossing) | 100 | 165 | 16.5 | 160 | 100 | 16.0 | 18 |
| Backlick Rd. (Near Interstate 95) | 95 | 190 | 18.0 | 140 | 125 | 17.5 | 25 |
| Annex (Paved Track) | 95 | 185 | 17.6 | 200 | 85 | 17.0 | 50 |
| Annex (20% Slope) | 95 | 160 | 15.2 | 30 | 475 | 14.25 | Creep |
| Backlick Rd. (Bank's Auto) | 95 | 185 | 17.6 | 190 | 90 | 17.1 | 39 |
| Backlick Rd. (Bottom of Hill) | 95 | 180 | 17.1 | 220 | 75 | 16.5 | 57 |
| Backlick Rd. (Near Airport) | 95 | 185 | 17.6 | 190 | 90 | 17.1 | 39 |
| Pohick Rd. & U. S. 1 | 115 | 60 | 6.9 | 115 | 60 | 6.9 | 30 |
| Pohick Rd. (Up Hill) | 100 | 160 | 16.0 | 100 | 160 | 16.0 | 15 |

d. Power Test 2. Power test 2 covered a distance of 31.9 miles paved surface with grades not in excess of 5 percent. A total of 6.5 gallons of hydrazine monohydrate was consumed during the test. The average power was 18 kilowatts for a total of 1.5 hours. This represents a fuel consumption of 4.9 miles per gallon or 1.338 pounds per kilowatt-hour, thus a fuel cell efficiency of 31 percent.

6. Component Tests. The following component tests were performed:

a. Fuel Cell Test. Tests conducted on the fuel cell power plant described in paragraph 4a revealed that the voltage for the 20-kilowatt system after 50 hours of operation decreased to 75 volts at 133 amperes in lieu of the 112 volts at 180 amperes. Thus the output power capability was reduced to approximately 50 percent of the design value.

The static controller described in paragraph 4c and the traction motor described in paragraph 4d were used to evaluate the effect of pulse loading on the fuel cell. The filter consisting of choke and capacitor shown in Fig. 8 were deleted from the circuit. Figure 17 shows fuel cell voltage and current, and Fig. 18 shows motor voltage and current. The fuel cell voltage dropped to approximately 70 volts during the period when current was supplied to the controller. The motor inductance was adequate to maintain continuous current flow into the motor. Additional tests were conducted with a hybrid power supply consisting of nickel-cadmium batteries in parallel with the fuel cell. The results are shown in Figs. 19 and 20. The load applied to the power supply was increased until the supply voltage decreased to an average of 85 volts. This resulted in a load of 2.3 times that applied to the fuel cell only. The transient effect of loading is approximately the same in either case. The regulation was improved by the addition of batteries.

The test was repeated with the filter choke and capacitor in the circuit. Figure 21 shows that the filter eliminates the effects of pulse loading as shown by the average current drawn from the power supply.

A 20-horsepower load condition at a vehicle speed of 4 miles per hour was applied to determine what influence the filter choke and filter capacitor have on the power supply voltage and current. Figure 22 shows negligible ripple on both voltage and current. Results shown in Fig. 23 were obtained with the filter choke removed. Negligible effect was noticed on the voltage. The current has both ringing and ripple. Figure 24 was taken with the filter choke and capacitor removed. The voltage at the time of conduction regulates from approximately 100 volts to 45 volts.

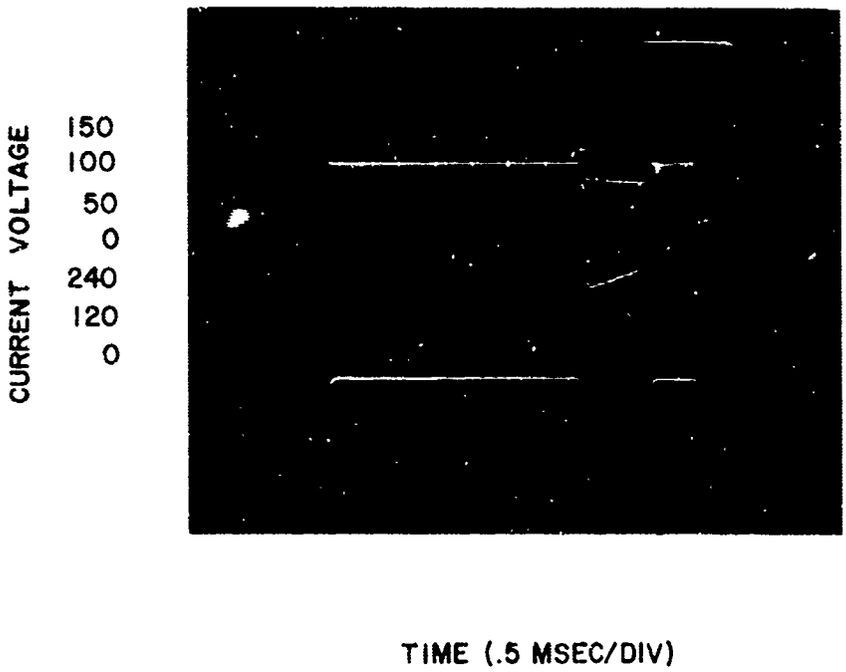


Fig. 17. Voltage and current of fuel cell with vehicle stationary.

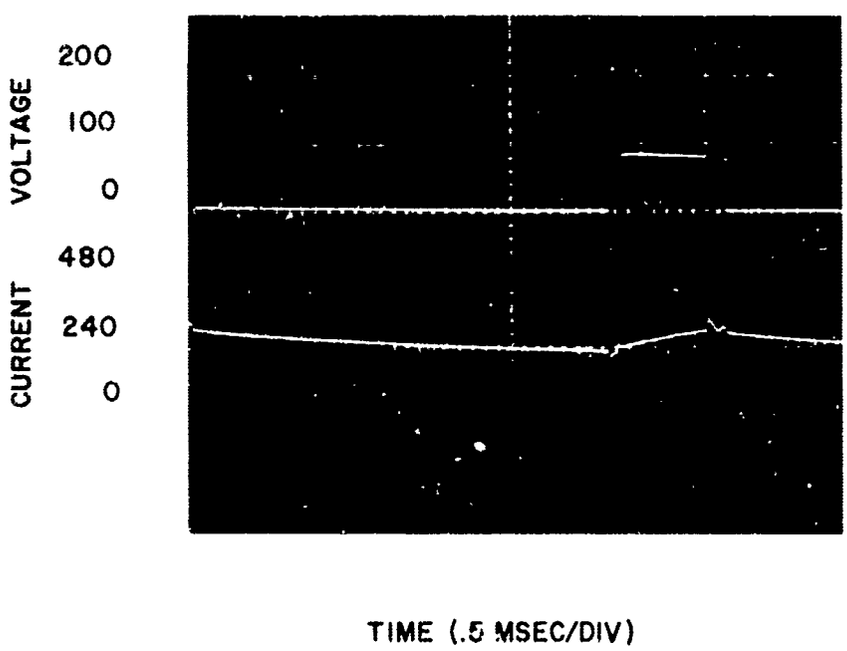


Fig. 18. Voltage and current of motor with vehicle stationary.

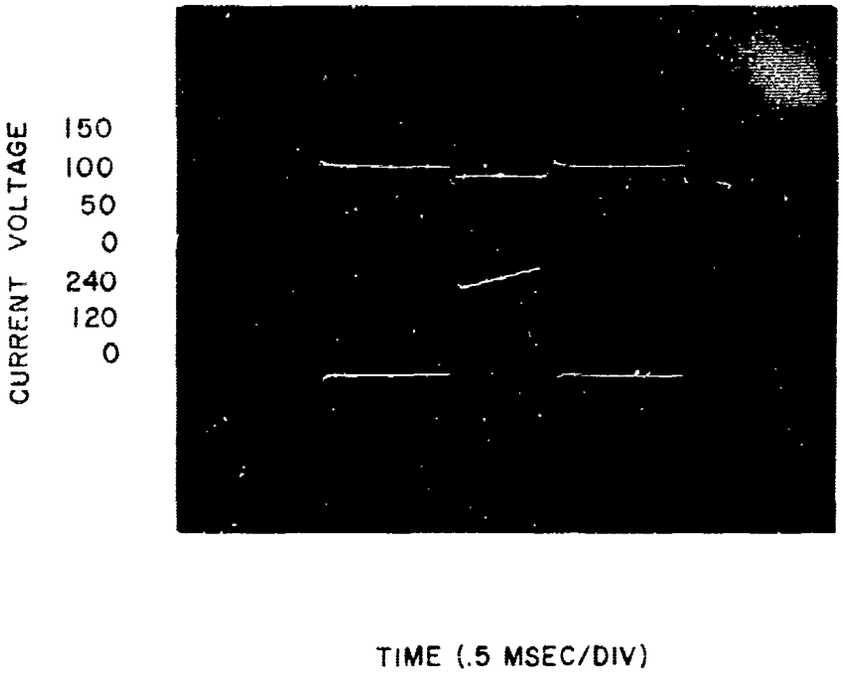


Fig. 19. Voltage and current of hybrid power supply without filter.

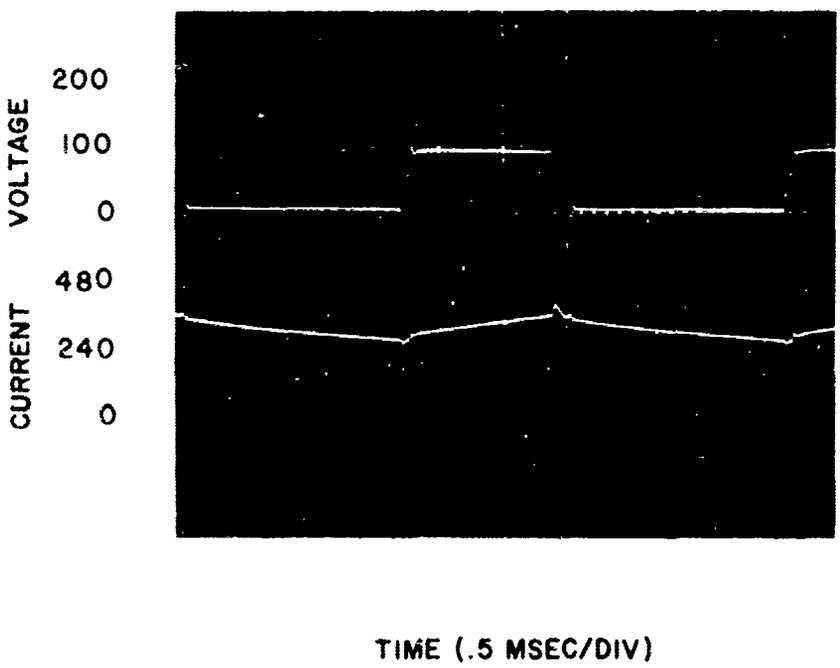


Fig. 20. Voltage and current of motor without filter.

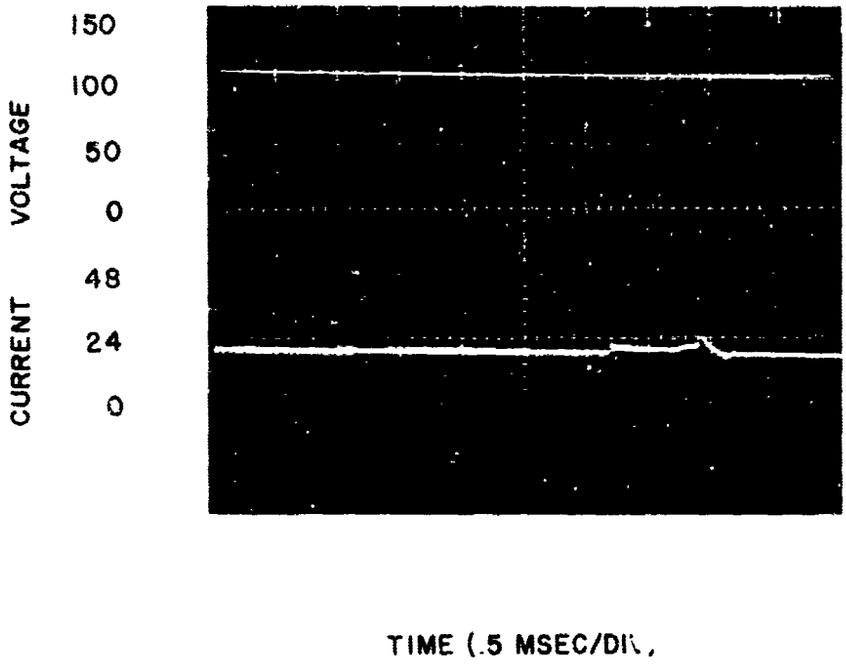


Fig. 21. Voltage and current of hybrid power supply with filter.

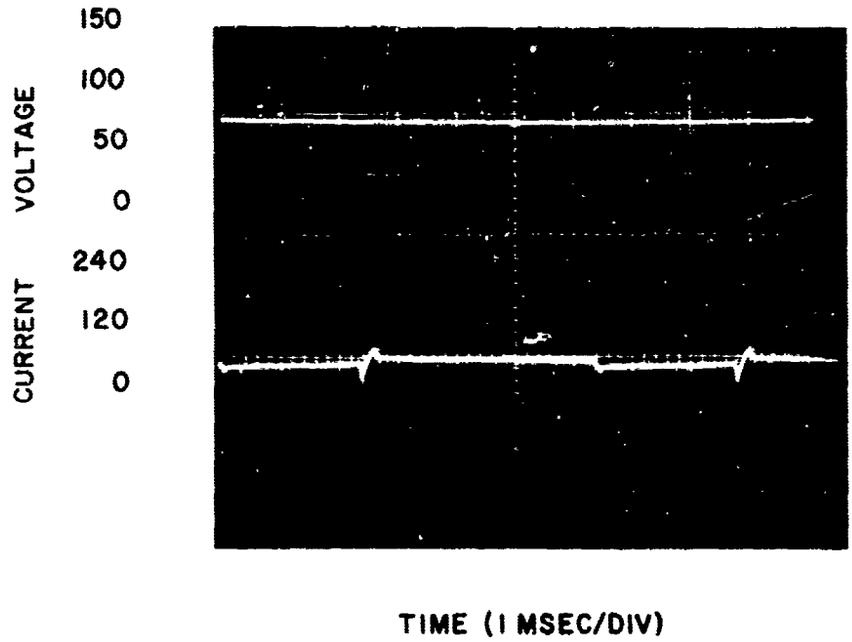


Fig. 22. Voltage and current of hybrid power supply with filter at vehicle speed of 4 miles per hour.

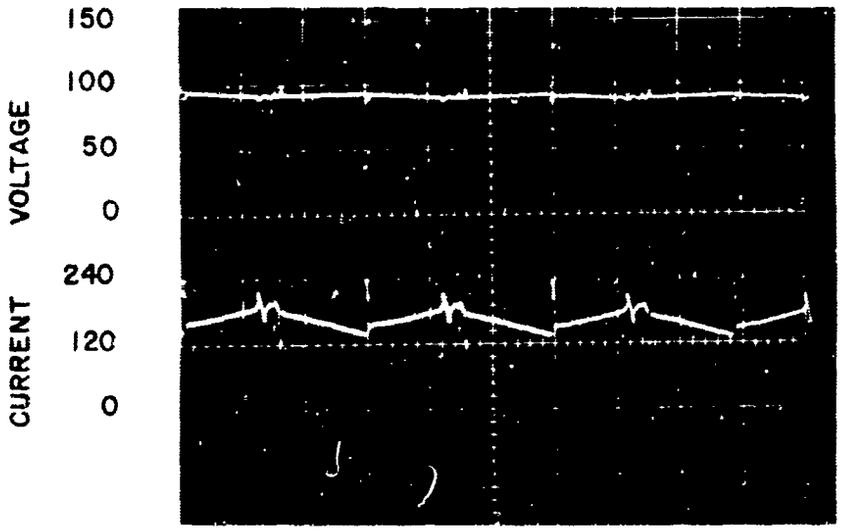


Fig. 23. Voltage and current of motor without filter at vehicle speed of 4 miles per hour.

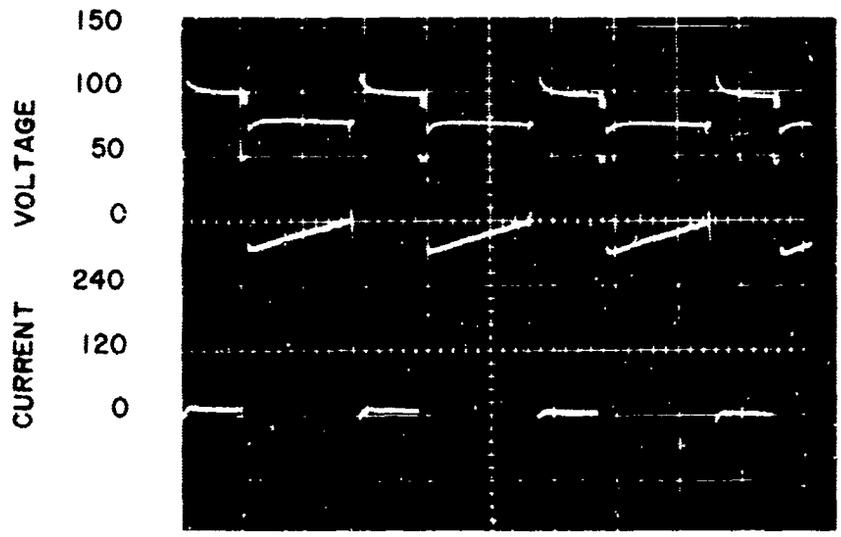


Fig. 24. Voltage and current of hybrid power supply without filter choke.

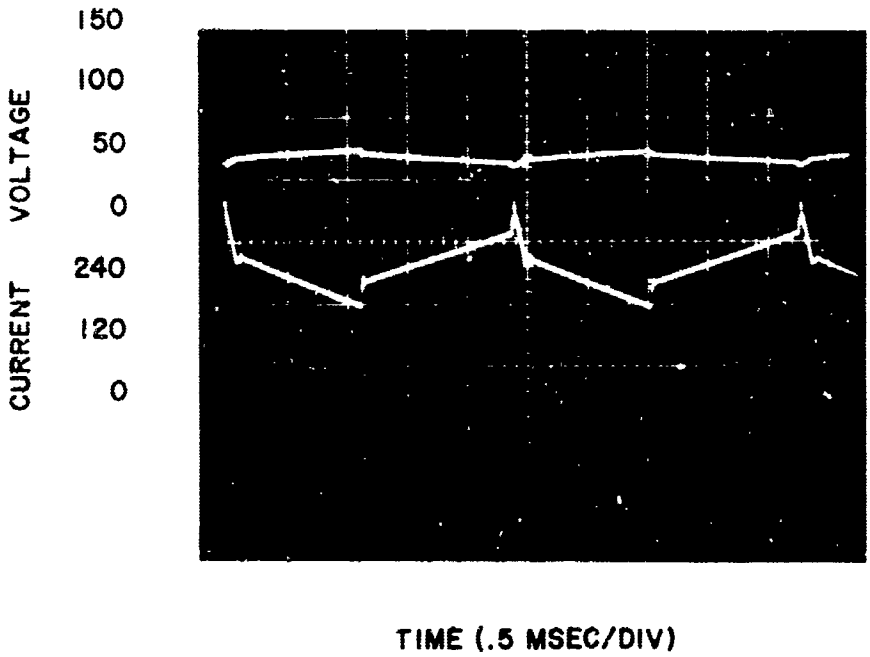


Fig. 25. Voltage and current of hybrid power supply with filter at vehicle speed of 30 miles per hour.

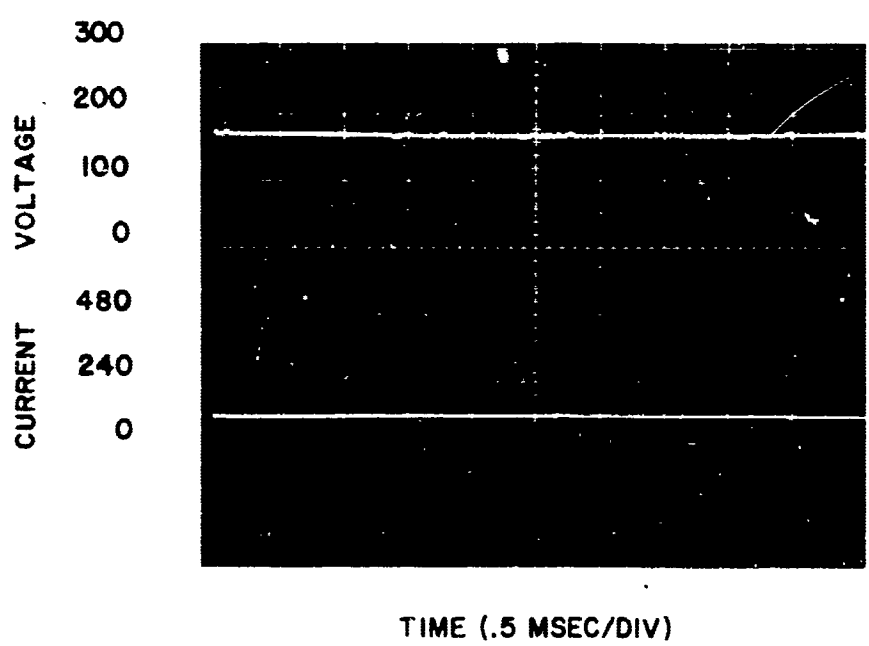


Fig. 26. Voltage and current of motor with filter at vehicle speed of 30 miles per hour.

The current peaks must be supplied to the load in lieu of an average value. Without the filter, it was noted that the load current capability was reduced since the amount of current that may be commutated is a function of the reverse voltage applied to the device. In the three conditions discussed, the filter reduced the detrimental effects of pulse loading and provided a higher output power capability.

The primary function of the filter choke and capacitor is to provide a greater motor voltage than is available at the supply. Figure 25 shows a 28-horsepower load condition at a vehicle speed of 30 miles per hour. Figure 26 shows that the motor voltage and current is a pure direct current. Although the voltage drops to 60 volts, the ripple content is rather low. The current has a saw tooth shape with a peak current of 420 amperes and minimum current of 300 amperes. The controller was designed to limit the average current drain to 360 amperes.

This series of tests have shown that the power source whether fuel cell or battery is significantly improved with the addition of a filter choke and capacitor. The transient and steady-state voltage regulation associated with pulse loading requires additional considerations.

b. Static Controller Test. Tests at 20 kilowatts were conducted with the traction motor described in paragraph 4d, and with an equivalent R-L load. Inspection of Table II shows a close correlation of the data. This makes acceptance of the tests shown in Table III reasonable. Selected load points were chosen to cover the full horsepower range of the controller. An inductance equal to that of the 1244 motor (1.7 millihenries) was connected in series. Data points were taken in the step-up and step-down modes for both input voltage (low voltage 112, high voltage 224) at full power and at reduced power. A load point was convenient for the high-voltage straight-through mode, but none was available for the low-voltage straight-through condition.

Figure 27 shows how closely the full power points for both voltage inputs fit a theoretical input curve to the 1244 motor to deliver 40 horsepower to the shaft at a motor efficiency of 90 percent. To keep the graph uncluttered, the reduced load points were not plotted. In general, the efficiency was above the 90-percent level.

Figure 28 shows the measured efficiencies at the full load points, and estimated curves are sketched in to indicate trends. One would expect the efficiency to be maximum at the straight-through condition. This was measured at 90 percent for the high-voltage connection.

Table II. Correlation Test Data

| Run No. | Mode of Operation | Static Controller Input | | 1244 Motor Input | | Dynamometer Output | | Speed (rpm) |
|---|---|---|---|---|---|---|---|---|
| | | Volts | Amperes | Volts | Amperes | Volts | Amperes | |
| 1 | Step-down | 112 | 200 | 58 | 342.5 | 66 | 134.4 | 270 |
| 2 | Straight-through | 115 | 160 | 110 | 160 | 49 | 206.4 | 840 |
| 3 | Step-up | 112 | 200 | 235 | 85 | 62.6 | 167.1 | 2,450 |
| | | | | R-L Load | | Resistance (Ω) | | Inductance (mh) |
| 4 | Step-down | 110 | 197.5 | 60 | 327.5 | 0.185 | | 1.7 |
| 5 | Straight-through | 113 | 167.5 | 105.5 | 166 | 0.62 | | 1.7 |
| 6 | Step-up | 111 | 185 | 233 | 80 | 2.68 | | 1.7 |
| | | | | R-L Load | | | | |
| 7 | Step-down | 110 | 200 | 60 | 325 | | | |
| 8 | Straight-through | 112 | 170 | 105 | 167.5 | | | |
| 9 | Step-up | 110 | 200 | 235 | 85 | | | |

Note: Runs 4 through 6 were conducted with the USAERDL controller.
Runs 7 through 9 were conducted with the breadboard controller.

Table III. Forty-Kilowatt Static Controller Test Data

| Point | Mode of Operation | Input | | Output | | Approx. Load Resist. (ohms) |
|---|---|---|---|---|---|---|
| | | Volts | Amperes | Volts | Amperes | |
| (1) | Step-down | 246 | 125 | 58.2 | 473 | 0.110 |
| 2 | " | 248.3 | 34.0 | 30.3 | 243 | 0.110 |
| (3) | " | 245 | 186 | 97.5 | 415 | 0.215 |
| 4 | " | 249.5 | 50 | 51.4 | 218.5 | 0.215 |
| (5) | Straight-through | 249 | 127 | 246.5 | 127 | 1.66 |
| (6) | " | 242 | 175 | 281 | 145 | 1.64 |
| 7 | Step-down | 248 | 50 | 135 | 75 | 1.64 |
| (8) | Step-up | 243.5 | 145 | 380 | 88 | 4.2 |
| 9 | " | 246.5 | 83.5 | 294 | 66.5 | 4.2 |
| (10) | " | 113.2 | 344 | 382 | 88.5 | 4.2 |
| 11 | " | 118.8 | 181.5 | 295 | 66.5 | 4.2 |
| 12 | " | 124 | 74 | 122 | 71.5 | 1.64 |
| (13) | " | 115 | 369 | 260 | 149.5 | 1.64 |
| 14 | " | 123.2 | 89.5 | 135 | 78.5 | 1.64 |
| 15 | Step-down | 125 | 33.5 | 81 | 46 | 1.64 |
| 16 | " | 116 | 325 | 94.3 | 376.5 | 0.215 |
| 17 | " | 122.7 | 99 | 53 | 212.5 | 0.215 |
| (18) | " | 114.7 | 367 | 100.2 | 393 | 0.215 |
| (19) | " | 116.4 | 302 | 65 | 500 | 0.125 |
| 20 | " | 123.5 | 71.5 | 33 | 250.5 | 0.125 |

Note: Points 1 through 9 on 240-volt input connection.
Points 10 through 20 on 120-volt input connection.
Circled points are full power.
R-L Load - L = 1.7 mh.

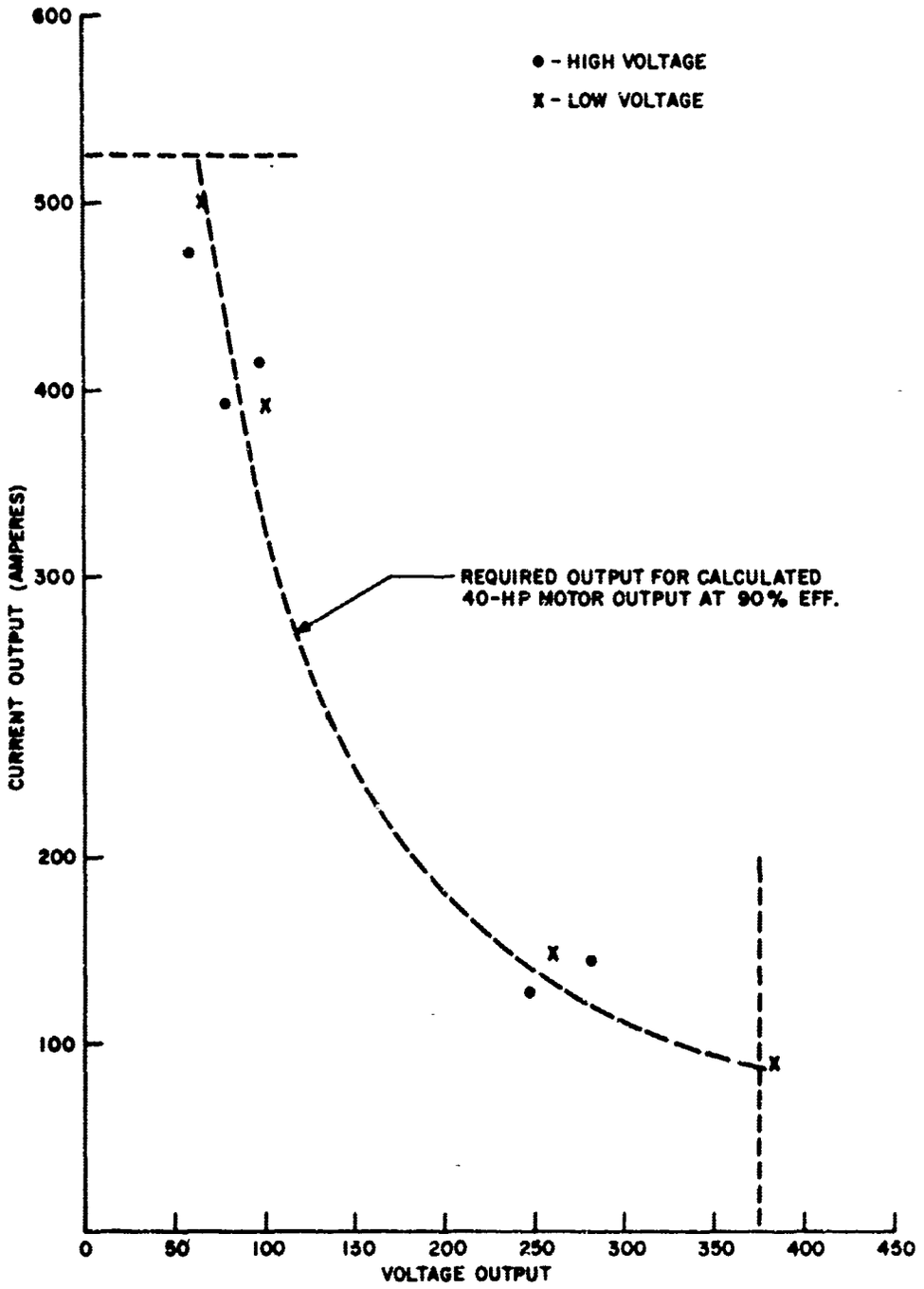


Fig. 27. Controller output current versus output voltage at 40-horsepower load.

Since the low-voltage connection essentially halves the voltage and doubles the current, one would expect at least 4 percent loss instead of 1 percent. It seems reasonable to predict that the wider the difference between output and input voltages, the lower will be the efficiency.

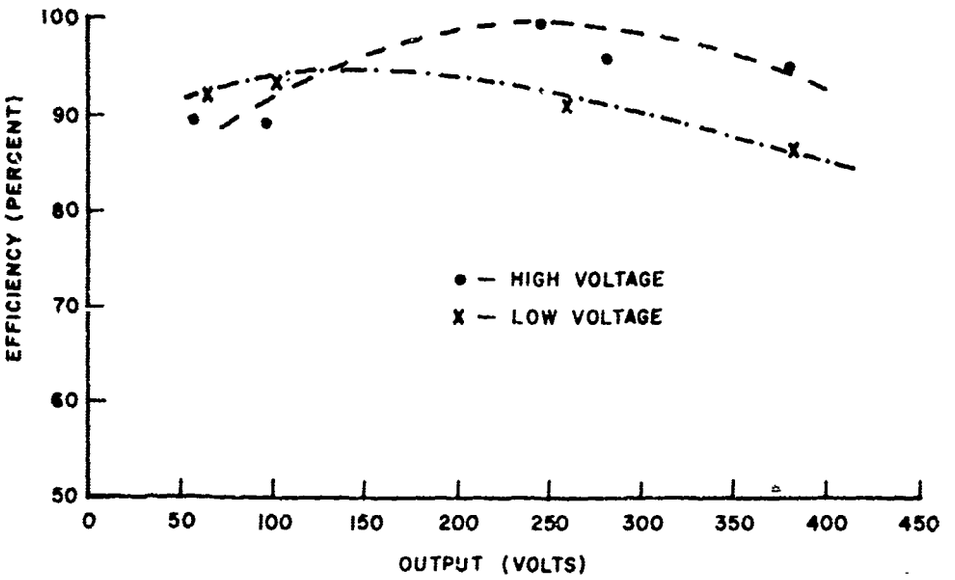


Fig. 28. Efficiency versus output voltage at 40-horsepower load.

c. Traction Motor Test. The motor characteristic curves shown in Fig. 29 provide the relationship of motor efficiency, speed, and torque as a function of motor current. By proper control of the motor, depending on the load, higher efficiencies are possible.

## III. DISCUSSION

7. Significance of the Project. As installed in the truck, the hydrazine-air fuel cell system (excluding the motor and controller) has a high energy density, nearly 350 watt-hours per pound for an 18-hour mission. For an 8-hour mission, the energy density drops to 210 watt-hours per pound, still much higher than is offered by any other readily available static system. The successful operation of the M-37 truck with a system having such a high power density must be considered an important step forward in the practical application of fuel cells.

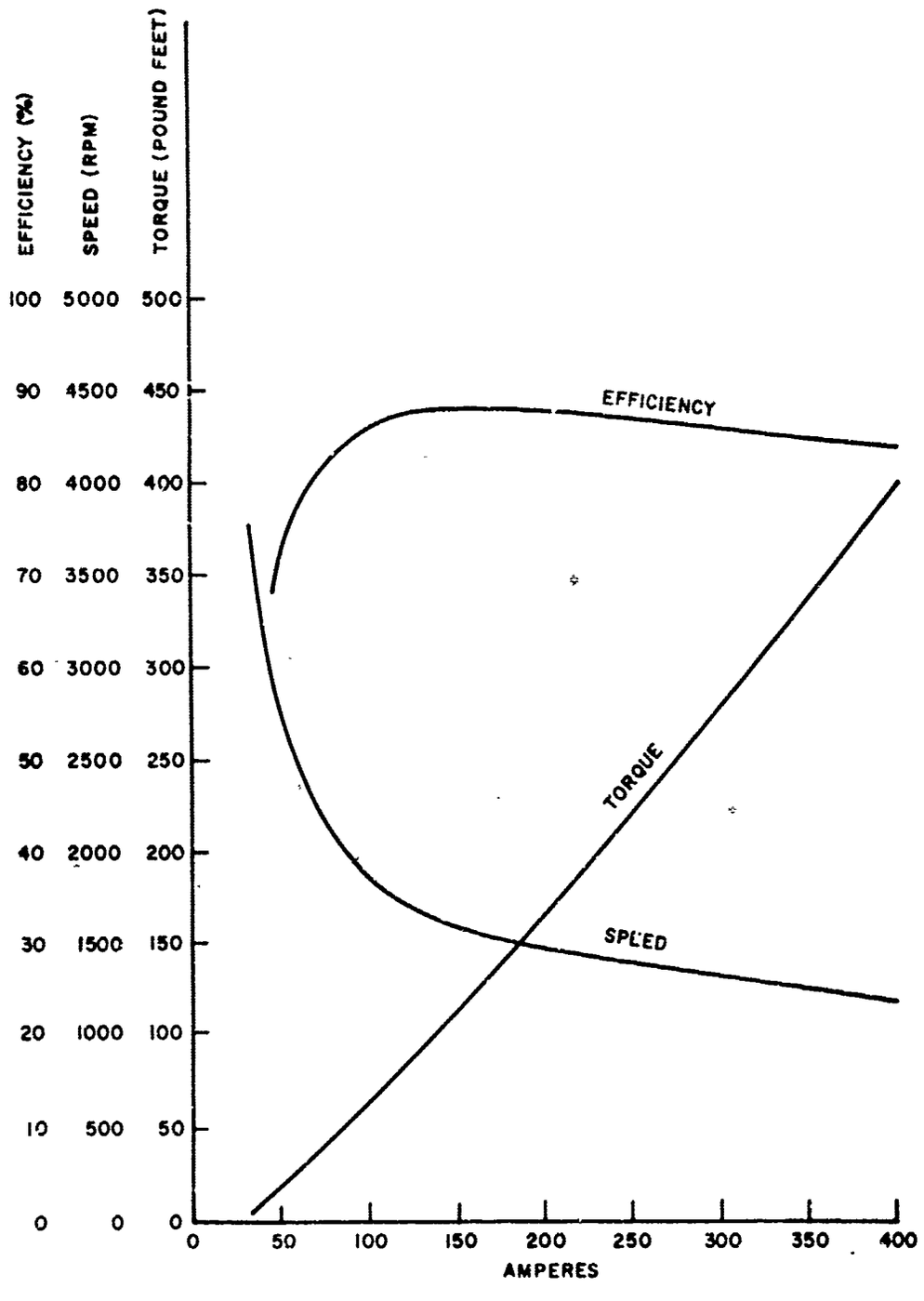


Fig. 29. Motor performance curves.

Valuable experience has been gained in the operation and control characteristics of an electric vehicle by using the hydrazine-air system. The relative simplicity and ease of operation of this large hydrazine-air fuel cell power plant has been demonstrated by over 100 operating hours in the truck.

8. Suggestions for Further Research and Development. A start has been made in applying fuel cells to military vehicle propulsion use. To make further progress, research and development must be continued and intensified.

A drastic reduction in the cost of platinum in the electrodes is required. If two 5-kilowatt modules as they presently exist are considered, and if reasonable reclamation and capital costs for the platinum are applied, annual expenditure of well over $500 is incurred by the use of this precious metal. Much work remains to be done, however, to optimize the platinum loading and to reduce the resulting electrode to a practical, reliable, and durable component.

Improvement of reliability and durability of the fuel cell is needed. In concept, the fuel cell promises to be highly reliable and very durable, matching and ultimately exceeding the lead-acid battery in these respects. The fuel cell of today has not lived up to this promise. However, in a relatively short time, great improvements have been made. Most first-order failure mechanisms have been identified and eliminated so that 1,000 hours of life is common on a single cell. Since this fuel cell battery contains 140 or 240 cells in a series, the problem of battery life is more severe than that of a single cell. Consequently, much work needs to be done to identify second-order life-limiting phenomena and to find ways to extend life and reliability. A goal of 1,000 hours of stack life is reasonable for the short-range development.

A reduction of specific weight is desired. Engineering studies have shown that a 10-kilowatt fuel cell module weighing only 75 pounds can be developed in the short term. Although optimistic, this goal can be reached by the application of sound engineering principles in a disciplined design effort.

Vehicle design incorporating the modularization concept provided by fuel cell and battery power plants should be accelerated to capitalize on new frame layouts, new suspension systems, new brake systems, etc.

Weight and cost reductions are required for the power conditioning equipment, and will be of a greater concern with multipowered wheel operation. Plans are underway to have four individual powered wheels on the next test rig (Fig. 30).

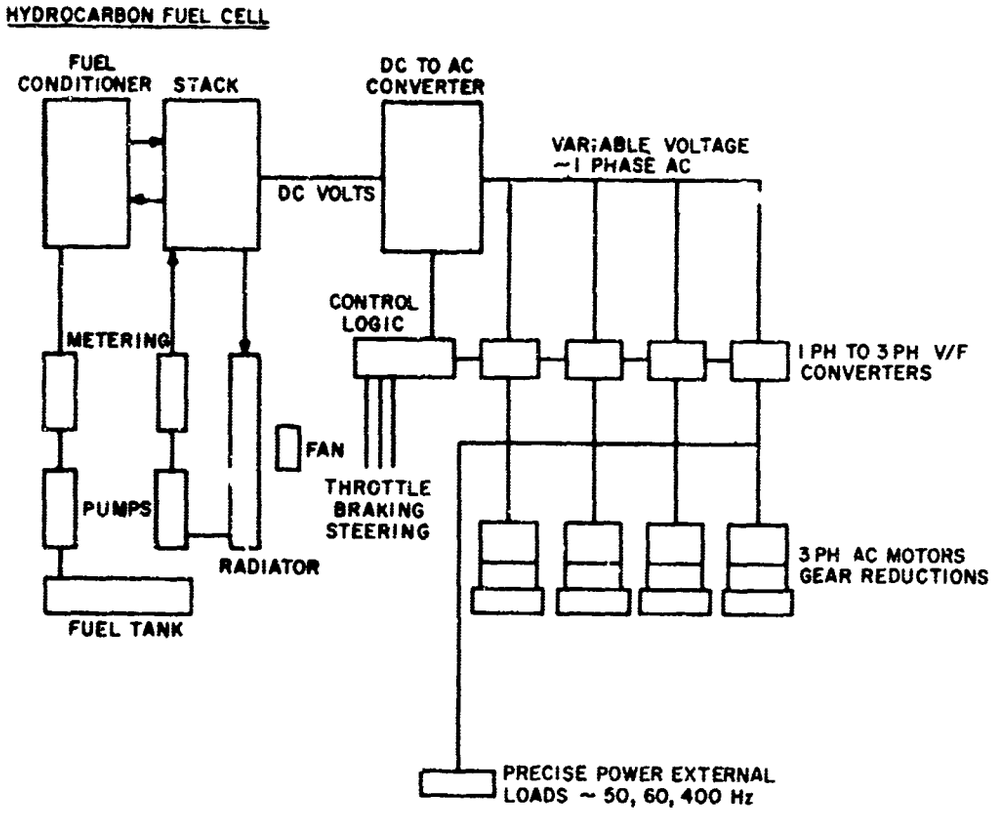


Fig. 30. Schematic of proposed fuel cell test rig.

Higher power density for the rotating equipment is required to enable motor-gear-wheel mounting. The unsprung weights and vehicle inertias are important considerations for optimization studies.

## IV. CONCLUSIONS

9. Conclusions. It is concluded that:

a. The fuel cell and electric drive as demonstrated are feasible for propulsion uses, but require additional research, development, and engineering.

b. The fuel cell-electric propulsion system performs satisfactorily for both highway and limited off-highway operation.

c. The use of a fuel cell as compared with other power plants such as a battery does not pose additional electrical problems.

d. Major technical advances are required to achieve military characteristics for similar vehicles.

UNCLASSIFIED

Security Classification

**DOCUMENT CONTROL DATA - R & D**

*(Security classification of title, body of abstract and indexing annotation must be entered when the overall report is classified)*

| | |
|---|---|
| 1. ORIGINATING ACTIVITY (Corporate author)<br>U. S. Army Mobility Equipment Research and Development Center<br>Fort Belvoir, Virginia 22060 | 2a. REPORT SECURITY CLASSIFICATION<br>Unclassified<br>2b. GROUP |

3. REPORT TITLE

FUEL CELL-ELECTRIC PROPULSION TEST RIG (MODIFIED M-37, 3/4-TON CARGO TRUCK)

4. DESCRIPTIVE NOTES (Type of report and inclusive dates)

Engineering Report July 1965 - December 1967

5. AUTHOR(S) (First name, middle initial, last name)

Lonnie D. Gaddy, Jr.

| 6. REPORT DATE | 7a. TOTAL NO. OF PAGES | 7b. NO. OF REFS |
|---|---|---|
| February 1968 | 50 | 1 |

| | |
|---|---|
| 8a. CONTRACT OR GRANT NO.<br>b. PROJECT NO.<br>c. Task No. 1C022001A01201<br>d. | 9a. ORIGINATOR'S REPORT NUMBER(S)<br>1921<br>9b. OTHER REPORT NO(S) (Any other numbers that may be assigned this report) |

10. DISTRIBUTION STATEMENT This document has been approved for public release and sale; its distribution is unlimited.

| | |
|---|---|
| 11. SUPPLEMENTARY NOTES | 12. SPONSORING MILITARY ACTIVITY<br>Department of the Army<br>U. S. Army Mobility Command |

13. ABSTRACT

This report covers a study to determine experimentally the feasibility and practicability of a fuel cell and electric drive propulsion system. The experimental data were obtained by testing the fuel cell test rig components and system.

The report concludes that:

a. The fuel cell and electric drive are feasible.
b. The fuel cell-electric propulsion system performs satisfactorily.
c. The use of a fuel cell as compared with other power plants such as a battery does not pose additional electrical problems.
d. Major technical advances are required.

DD FORM 1 NOV 65 1473 REPLACES DD FORM 1473, 1 JAN 64, WHICH IS OBSOLETE FOR ARMY USE.



UNCLASSIFIED

Security Classification

| 14. KEY WORDS | LINK A | | LINK B | | LINK C | |
|---|---|---|---|---|---|---|
| | ROLE | WT | ROLE | WT | ROLE | WT |
| Fuel cell<br>Power source<br>Electric drive<br>Static controller for direct-current motors | | | | | | |